Engineering Division
IIT Research Institute
10 West 35th Street
Chicago, Illinois 60616

Fourth Interim Report

Contract F44620-75-C-0059

IITRI Project J6352

INITIATION MECHANISMS OF SOLID ROCKET PROPELLANT DETONATION

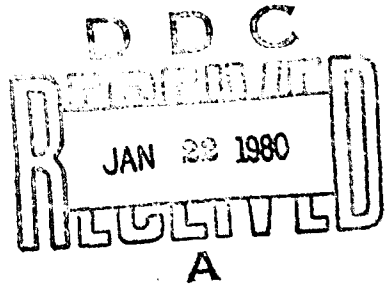

Prepared by
A. N. Takata

for

Air Force Office of Scientific Research
Bolling AFB, DC 20332

November 1979

SECURITY CLASSIFICATION OF THIS PAGE (When Data Entered)

REPORT DOCUMENTATION PAGE

READ INSTRUCTIONS BEFORE COMPLETING FORM

1. REPORT NUMBER: AFOSR-TR-79-1324	2. GOVT ACCESSION NO.
3. RECIPIENT'S CATALOG NUMBER	
4. TITLE (and Subtitle): INITIATION MECHANISMS OF SOLID ROCKET PROPELLANT DETONATION	5. TYPE OF REPORT & PERIOD COVERED: FINAL, 1 Jan 75 - 30 Sep 79
6. PERFORMING ORG. REPORT NUMBER: J6352	
7. AUTHOR(s): A. N. TAKATA	8. CONTRACT OR GRANT NUMBER(s): F44620-75-C-0059
9. PERFORMING ORGANIZATION NAME AND ADDRESS: IIT RESEARCH INSTITUTE, 1C WEST 35th STREET, CHICAGO, ILLINOIS 60616	10. PROGRAM ELEMENT, PROJECT, TASK AREA & WORK UNIT NUMBERS: 2308A1, 61102F, A1
11. CONTROLLING OFFICE NAME AND ADDRESS: AIR FORCE OFFICE OF SCIENTIFIC RESEARCH/NA, BLDG 410, BOLLING AIR FORCE BASE, D C 20332	12. REPORT DATE: Nov 79; 13. NUMBER OF PAGES: 54
14. MONITORING AGENCY NAME & ADDRESS (if different from Controlling Office): IITRI-J6352-FR	15. SECURITY CLASS. (of this report): UNCLASSIFIED
	15a. DECLASSIFICATION/DOWNGRADING SCHEDULE

16. DISTRIBUTION STATEMENT (of this Report)

Approved for public release; distribution unlimited.

17. DISTRIBUTION STATEMENT (of the abstract entered in Block 20, if different from Report)

Interim report no. 4 (Final) 1 Jan 75 - 30 Sep 79,

18. SUPPLEMENTARY NOTES

19. KEY WORDS (Continue on reverse side if necessary and identify by block number)

DEFLAGRATION TO DETONATION TRANSITIONS (DDT)
ROCKET MOTOR DETONATION
NUMERICAL METHODS
PROPELLANTS

20. ABSTRACT (Continue on reverse side if necessary and identify by block number)

The purpose of this study is to identify mechanisms responsible for several accidental detonation of high-energy solid rocket propellant motors. During the past year a computer model was developed to predict the amount of foam or melt generated in cracks following sudden exposure of the crack to a cavity containing higher temperature/pressure gases than exists within the crack. In addition an experimental design was developed to study deflagration to detonation transitions (DDT). Analytical predictions suggest that DDT can occur as a consequence of burning propellant cracks provided molten propellant is generated within the

DD FORM 1 JAN 73 1473 EDITION OF 1 NOV 65 IS OBSOLETE

UNCLASSIFIED

burning propellant cracks and the cracks are subjected to sufficiently high amplitude stress waves. The stronger the stress waves are, the less the amount of melt needed for DDT. DDT can be initiated by single burning cracks in close proximity to the motor case, or by multiple burning cracks which are similarly oriented by respect to each other and closely spaced.

FOREWORD

The objective of this project is the understanding of the mechanisms controlling the transition from deflagration to detonation in solid propellant rocket motors. This interim report covers the period from October 1978 through September 1979. The study was sponsored by the Air Force Office of Scientific Research (AFOSR), Directorate of Aerospace Sciences, United States Air Force under Contract F44620-75-C-0059. The program was monitored by Captain R. F. Sperlein of AFOSR.

IIT Research Institute personnel who contributed to this research are H. S. Napadensky, A. N. Takata, and A. H. Wiedermann.

Respectfully submitted,
IIT RESEARCH INSTITUTE

A. N. Takata

A. N. Takata
Senior Research Engineer

APPROVED:

T. E. Waterman
Engineering Advisor
Manager, Fire and Safety Research

CONTENTS

ILLUSTRATIONS

TABLES

1. INTRODUCTION

In recent years high-energy propellants have been developed containing cyclotetramethylenetranitramine (HMX) to improve the performance of rocket motors. In testing such propellants, several accidental explosions have occurred during rocket motor firings. The goal of this study is the identification of the causes of the explosions in order to prevent such occurrences in the future.

This program examines possibilities of deflagration to detonation transitions (DDT) caused by sudden exposure of cracks to high pressure/temperature gas cavities such as the combustion chamber. It consists of the following steps:

- development of analytical means with which to identify crack conditions and propellant properties needed to produce pronounced/rapid pressure rises within burning cracks
- comparison of predicted pressure transients with stepwise shock wave amplitudes and durations known to initiate propellants, and
- validation of analytical predictions by experimental means.

Results of previous IIT Research Institute (IITRI) studies are described in references [1] through [4].

1.1 Background

During previous IITRI studies two factors were identified as possible causes of pronounced pressure rises. Namely stress waves that partially collapse burning cracks, and foam or melt layers that are rapidly consumed by dynamic burning. Stress waves are generated by rapid pressure rises within cracks. They may be produced by sudden exposure of cracks to high-pressure gas cavities and/or rapid burning of the propellant within the cracks. The consequence of applying stress waves to a burning crack is stress waves of appreciably greater amplitude. Resultant stress waves will then compress any neighboring burning cracks and produce stress waves of still higher amplitude. By

this process, progressively more pronounced pressures can be generated within neighboring burning cracks on a crack by crack basis.

Pressure rises are also highly dependent upon the foam mass and temperature, and upon the size and orientation of the cracks with respect to each other. With foam masses of the order of 0.01 g/cm^2 or greater, only a few parallel closely spaced burning cracks are needed to achieve pressures of the order of 10 kbars. Much of the pressure rise occurs within a fraction of a μsec.

1.2 Status of Present Study

The scope of work for the present study consisted of the following analytical and experimental tasks:

(1) Measurement of HMX foam mass present during steady burning at ambient pressure

(2) DDT experiments in which burning propellants are impacted by a flyer plate

(3) Incorporation of pressure-dependent propellant impedance in computerized models

(4) Prediction of transient pressures produced sequentially within a series of burning cracks

(5) Development of a computer code with which to predict amounts of foam or melt generated within cracks suddenly exposed to cavities containing high temperature/pressure gases

No sources of HMX cylinders with dimensions of the order of several centimeters could be found. Thus 20 cylinders of propellant composed of approximately 65 percent HMX and 35 percent polyethlylene glycol binder were ordered in May 1979 for the foam mass and DDT experiments cited by items 1 and 2. Unfortunately the propellant cylinders were not received in time to conduct the experiments. Instead efforts were expended in:

- upgrading the experimental design described in the previous interim report [4],
- assessing the effect of sudden pressure relief upon foam masses present during steady burning,
- assessing rates of temperature rise of gases evolved by heated HMX prior to ignition, and
- analyzing means for predicting the ignition of HMX.

Items 3 through 5 have been completed and resulted in two computerized models called PROS and PROP. PROS is a new code that predicts dynamic burning, melt formation, crack deformation and gas pressures along the length of cracks following sudden exposure to high-pressure gas cavities. Figure 1(a) illustrates the problem treated by PROS. Gases initially within the crack are at a state of rest with a uniform pressure and temperature. Initial crack widths may be uniform or variable along the length of the crack. Gas flows within the crack are treated as one-dimensional. Gas parameters and burning conditions, will of course, vary with crack location and time after the crack propagates into the cavity.

PROP is a revised edition of the code used in the previous interim report [4]. It predicts dynamic burning, crack deformations and gas pressures produced within an element of a burning crack subjected to stress waves. Amounts of gas escaping from the crack element are considered insignificant over the times of interest. During the past year a subroutine was incorporated into this model in order to guide development of the DDT fixture. The subroutine includes provisions for accounting for:

- generation of a system of plane stress waves radiating from the burning crack,
- reflection of the radiating stress waves by a high-density media such as the motor case,
- partial compression of the crack by the returning stress waves, and
- subsequent expansion of the crack by elevated gas pressures produced within the crack.

The remainder of this report describes basic analytical techniques used by the two models, the revised DDT fixture, and various predictions derived from the analytical studies. Nomenclature and property data are presented in the appendix at the rear of this report.

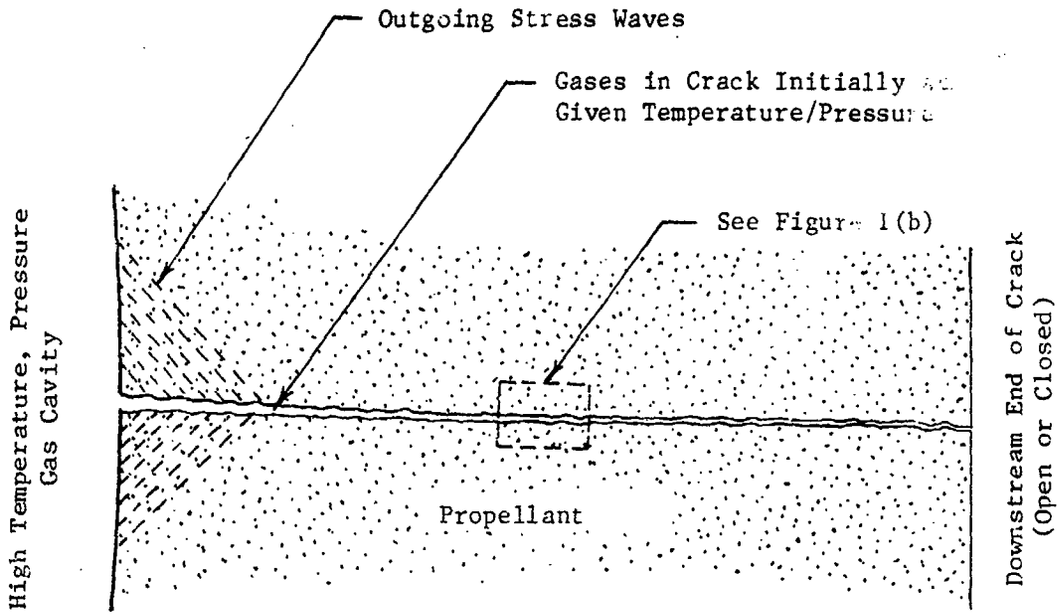

Figure 1(a). Crack Configuration Treated by PROS

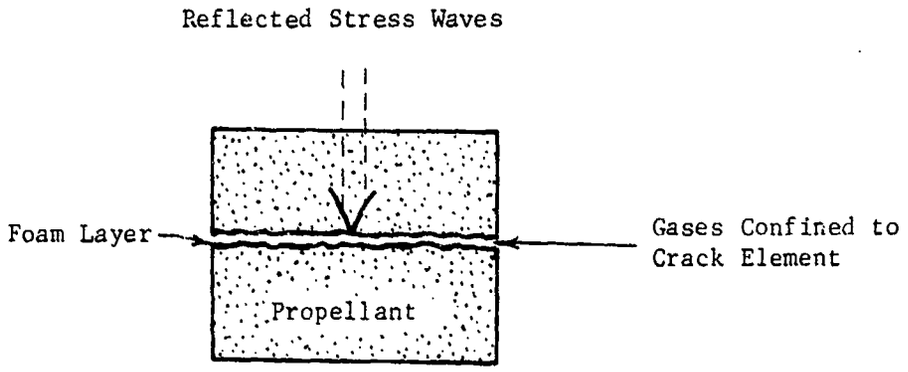

Figure 1(b). Crack Configuration Treated by PROP

2. BASIC EQUATIONS AND ANALYTICAL RESULTS

This section briefly describes means by which various phenomena are treated. Also included are a:

- discussion of ignition criteria, and
- predictions of changes in the foam mass of steadily burning HMX following sudden pressure relief.

2.1 Propellant Heating

Rates of propellant burning depend upon the temperature profile within the propellant, which in turn depends upon the time-dependent heat fluxes supplied the propellant before and following the start of burning. Systems of equations [4] are used to predict dynamic burning in terms of the heat fluxes received by the propellant crack surfaces.

This section is concerned with describing heat-flux expressions developed for PROS. In this regard, the equations used by PROP are special cases of the equations used by PROS. Heat fluxes, will of course, vary with the physical condition of the propellant surface, i.e., solid, melting or burning.

2.1.1 Convective Heat Flux q Prior to Start of Melting

Prior to the start of melting, the incident convective heat-flux q is described by the expression used by Kuo [5]. In terms of the gas temperature T_g and the temperature T_f of the propellants surface, the heat flux q is

$$q = h_c(T_g - T_f) \tag{1}$$

where the heat transfer coefficient h_c is given by

$$h_c = \frac{0.547 C_g M_w^{0.1} (Pu)^{0.8}}{P_r^{0.6} R^{0.8} T_g^{0.67} (LC_w)^{0.1}} \tag{2}$$

The dynamic heat flux q described by equations (1) and (2) is used in PROP. A constant heat flux q_s is used in PROP.

2.1.2 Heat Flux q_f During Melting

Two sources of heat flux are present while the propellant surface is melting. The first is the heat flux q described in subsection 2.1.1; the second is heat generation within the melt or foam layer. The latter is termed internal heating. While the propellant is melting prior to burning, the heat flux q_f is described by

$$q_f = q + \rho\, r_f\, Q_s \tag{3}$$

The term q represents the incident heat flux, while the second expression represents internal heating. In that the incident heat flux is convective it will decrease as the foam temperature T_f rises. On the other hand, increased foam temperature accentuates internal heating by raising the propellants regression rate r_f. The latter points up the importance of internal heating in speeding the melting of the propellant and in accelerating subsequent burning.

2.1.3 Heat Flux q_f During Burning

Gases evolved by burning propellants interact with gases flowing laterally along crack surfaces, and thereby perturb the convective heat fluxes cited earlier. Heat fluxes resulting from the interaction of the two gas flows are termed erosive. In this regard, Lenoir and Robillard [6] developed an expression for the rate $\bar{r}_f$ of steady burning produced by erosive heating. Subsequently their expression was used by Kuo [5]. It is given by

$$\bar{r}_f = a\, P^n + k\, h_c \exp\left(-\frac{\beta \rho \bar{r}_f}{\rho_g u}\right) \tag{4}$$

Since then King [7] upgraded the first expression on the right-hand side of equation (4) to account for the effect of erosive burning upon the flame standoff distance. The result is

$$\bar{r}_f = \frac{(aP^n)^2}{\bar{r}_f} + k h_c \exp\left(-\frac{\beta\rho\bar{r}_f}{\rho_g u}\right) \tag{5}$$

During steady burning, the heat flux $\bar{q}_f$ must maintain the foam temperature at a steady value $\bar{T}_f$ so that

$$\bar{q}_f = \rho\bar{r}_f[C_p(T_m - T_o) + C_m(\bar{T}_f - T_m) + Q_m] \tag{6}$$

For purposes of brevity, the expression within the brackets of equation (6) shall be represented by $\bar{Q}_f$. Multiplying equation (5) by $\rho\bar{Q}_f$ and replacing $\rho\bar{r}_f\bar{Q}_f$ by its equivalent $\bar{q}_f$ yields

$$\bar{q}_f = \frac{\rho(aP^n)^2\bar{Q}_f}{\bar{r}_f} + k h_c \exp\left(-\frac{\beta\rho\bar{r}_f}{\rho_g u}\right)\rho\bar{Q}_f \tag{7}$$

When the cross-flow gas velocity u is zero, the second expression on the right-hand side of equation (7) vanishes and the steady heat flux $\bar{q}_f$ equals the first expression given by equation (7).

In order to describe the heat flux q_f present during dynamic burning, we shall replace the first expression on the right-hand side of equation (7) by the expression developed by Krier [8] for dynamic burning as follows:

$$\frac{\rho(aP^n)^2\bar{Q}_f}{\bar{r}_f} \longrightarrow \frac{\rho(aP^n)^2(\bar{Q}_f - Q_s)}{r_f} + \rho r_f(\rho r_f Q_s)$$

$$\rho r_f(C_m - C_g)(T_f - \bar{T}_f) \tag{8}$$

Notice that the above expressions are identical for steady burning wherein $r_f = \bar{r}_f = aP^n$ and $T_f = \bar{T}_f$.

According to Lenoir and Robillard [6] the factor k given in equation (7) equals

$$k = \frac{(T_g - T_f)}{\rho \bar{Q}_f} \tag{9}$$

Substituting the expressions given by equations (8) and (9) into equation (7), and replacing $\bar{q}_f$ and $\bar{r}_f$ by their unsteady values q_f and r_f yields

$$q_f = \frac{\rho(aP^n)^2(\bar{Q}_f - Q_s)}{r_f} + \rho r_f Q_s + \rho r_f (C_m - C_g)(T_f - \bar{T}_f) +$$

$$h_c(T_g - T_f)\exp(-\frac{\beta \rho r_f}{\rho_g u}) \tag{10}$$

The dimensionless constant β of equation (10) must be evaluated experimentally. In that its value for HMX is not known to the author it shall tentatively be assumed equal to the value 15 determined by King [7] for a propellant different from HMX.

2.2 Dynamic Flow of Gases Within Cracks

An essential aspect of the problem is the prediction of the transfer of gases and heat along the length of a crack. For this purpose a gas dynamic model was developed [1]. It is based upon an Eulerian representation of the flow region and is limited to a one-dimensional treatment. The Eulerian representation was selected in that it permits simple identification of crack location and allows for mixing of freshly burnt reaction gas.

One-dimensional treatment is appropriate in that crack thicknesses and lengths are usually large compared to their width. Thus the most significant flow gradients and movements occur along the length of the crack. Values used in the one-dimensional treatment represent cross-sectional values.

The model treats a crack with a specified width variation at zero time. The gas in the crack at zero time is considered to have the same composition as the reaction products, and to

exist in a rest state at some uniform temperature and pressure. The crack is then suddenly connected to a cavity filled with gaseous reaction products at high temperature and pressure. The cavity state is treated as constant with respect to time due to the relatively short duration of the events occurring within the crack.

The downstream end of the crack can be either closed or connected to another cavity held at a specified pressure. In either case crack length is held constant.

2.3 Mechanical Deformation of Cracks

There are two sources of mechanical response of cracks. The first is elevated gas pressures within cracks that act to expand cracks. The second is due to stress waves radiating from cracks and subsequently interacting with other cracks or the same crack following interaction of the radiating stress waves with the confining shell structure.

The mechanical response of the propellant mass to pressures within cracks is very complex due to the multiplicity of stress wave types and the complex geometry of the crack, propellant mass and confining shell. The primary motion of the propellant mass will be in a direction normal to the crack and will be roughly one of plane strain. For this reason a simple local plane strain representation for the transient stress field was adopted in the absence of remote boundary effects.

A simple shell response model was selected to treat the remote boundary effect upon reflected stress waves. The model treats the shell as a simple single degree-of-freedom lumped mass which is position restrained and which responds to the mean radiative stress field. The response generates a system of reflected stress waves which arrive back at the crack after a delay period which depends upon the distances to the remote boundary.

Equations describing the velocities of the two crack walls caused by gas pressures and incident stress waves are presented in the previous interim report [4].

2.4 Ignition Criteria and Foam Mass

2.4.1 Ignition Criteria

Ignition refers to the start of propellant burning. Knowledge of when ignition occurs is important in that the heat flux undergoes rapid change following ignition.

Ignition represents a complex phenomenon which we attribute to exponential temperature rises of the evolved reaction gases caused by exothermic decomposition. If the above hypothesis is true then ignition depends upon:

- temperature, composition and flow rates of the gases evolved by the heated propellant, and
- physical and thermal environment into which the gaseous products are discharged.

Fortunately, as will be seen later in this section, one need not analyze each of the above phenomena to approximate ignition times. Nevertheless one should be aware of the phenomena in designing experiments with which to establish ignition criteria for the propellant/conditions of interest.

At present, ignition criteria are based upon propellant temperature, or combinations of a constant incident flux and duration [9]. The former criterion is of greatest value in that it applies to time-dependent heat fluxes. Ignition is predicted when the temperature of the propellants surface or at some depth exceeds a critical temperature.

In the remainder of this section we shall examine the effect of disregarding gas evolution upon the ignition time. Before doing so it should be noted that a one-to-one correspondence does not exist between foam temperature and rates of gas evolution.

Table 1 presents predicted foam temperatures following exposure of HMX to specified incident heat fluxes. Internal heating is also provided for even though it is not specified in the table. The initial temperature of the propellant is 294 K. Foam or propellant surface temperatures are specified at times at which the gas evolution rates equal specific fractions δ of the steady burning rate of 0.03 cm/sec.

TABLE 1. PREDICTED FOAM TEMPERATURES AND REGRESSION RATES OF HEATED HMX

Incident Heat Flux*, cal/cm^2-sec	Temperature T_f corresponding to specified fraction δ of the steady burning rate, K**				
	$\delta = 0$	$\delta = 0.1$	$\delta = 0.5$	$\delta = 0.9$	$\delta = 1.0$
0.5	555.0 (211.44)	565.6 (237.19)	580.9 (239.33)	587.7 (239.58)	588.9 (239.60)
1.0	555.0 (52.86)	570.30 (61.99)	585.9 (64.45)	589.1 (64.71)	592.3 (64.74)
2.0	555.0 (13.25)	579.0 (16.50)	588.9 (18.25)	594.9 (18.50)	596.1 (18.53)
10.0	555.0 (0.529)	603.5 (0.668)	607.8 (0.875)	611.6 (0.959)	612.4 (0.974)
30.0	555.0 (0.0587	629.1 (0.0697)	630.4 (0.0902)	631.8 (0.1031)	632.2 (0.1057)
100.0	555.0 (0.00529)	665.6 (0.00577)	664.5 (0.00681)	664.5 (0.00760)	664.6 (0.00770)

* Incident heat fluxes are from some external heat source.
** Times of occurrence given in parentheses in seconds.

From Table 1 it may be observed that an ignition criterion based solely upon a given temperature implies that ignition occurs with differing rates of gas release. The latter reemphasizes the question raised earlier regarding the significance of the differing rates of gas evolution upon the ignition time.

In order to perform the above assessment we shall assume that the critical ignition temperature lies between the melt temperature of 555 K and the lowest temperature cited in Table 1

for $\delta = 1$. A δ value of 1 is chosen since it corresponds to a regression rate equal to the steady burning rate. Based upon the above assumptions, the critical temperature lies between 555.0 and 588.9 K.

Applying the above temperature range to Table 1 indicates that the ignition time is between 211.4 and 239.6 sec when the incident flux is 0.5 cal/cm^2-sec; and between 0.00529 and a linearly interpolated value of 0.00544 sec when the incident flux is 100 cal/cm^2-sec. Notice that the above times differ by only 13.3 and 2.8 percent for the two fluxes. These results suggest that ignition temperature provides a reasonably accurate means for predicting ignition at least for HMX. Rates of gas evolution are of secondary importance.

For the present we shall assume that the ignition temperature of HMX equals the mean temperature (572 K) associated with the range of temperatures cited earlier. Ignition times t_i required to achieve a foam temperature of 572 K may be determined from Table 1 as a function of q. They are given approximately by

$$t_i = 59/q^2 \tag{11}$$

where t_i is in seconds when q is in cal/cm^2-sec. Experimental results presented in reference [9] indicate that the exponent 2 of equation (11) can vary from about 1.6 to 2.0 depending upon the propellant. Most propellants involve coefficients only a fraction of the coefficient 59 presented by equation (11). The relatively large coefficient is attributed to the high melt temperature of HMX and the fact that much of the "ignition time" is expended in initiating melting. In this regard, times to initiate melting are proportional to the square of the difference between the melt temperature and the initial temperature of the propellant [10].

2.4.2 Effect of Sudden Pressure Relief Upon HMX Foam Mass

In the previous interim report [4], Boggs' experimental results [11] were used to deduce the amount of HMX foam present during steady burning as a function of pressure. Foam masses were then used to evaluate the heat transfer coefficient associated with heat flow from the foam to the melt interface.

Foam masses were deduced by estimating the thickness and density of "frozen" HMX layers presented by Boggs [11]. Freezing was accomplished by suddenly relieving the pressure (34 and 68 bars) present during steady burning. Questions regarding the correspondence between the mass of "frozen" foam with the foam mass present during steady burning were not addressed. In other words, how much does the foam mass change following pressure relief due to continued outgassing and melting?

Figure 2 presents analytical predictions of the foam mass (molten plus frozen) as a function of time following sudden relief of the two pressures cited earlier. At time zero the foam mass equals that of steady burning. Several hundred milliseconds after pressure relief the foam is completely frozen.

It may be observed that the foam mass at 34 bars decreases from 0.00254 to 0.00220 g/cm^2 following pressure relief, while the foam mass at 68 bars decreases from 0.00139 to 0.00112 g/cm^2. Percentagewise, the above mass reductions are 13.4 and 19.4 percent, respectively. The somewhat greater reduction (percentagewise) of the foam mass present at 68 bars is due to its higher temperature. The result is more rapid mass loss of initially smaller amounts of foam.

While the above mass changes are significant, they are probably small compared to errors in estimating the thickness and density of the "frozen" foam. For this reason, the foam masses presented in the previous interim report [4] shall not be corrected until better measurements of the "frozen" foam mass are available.

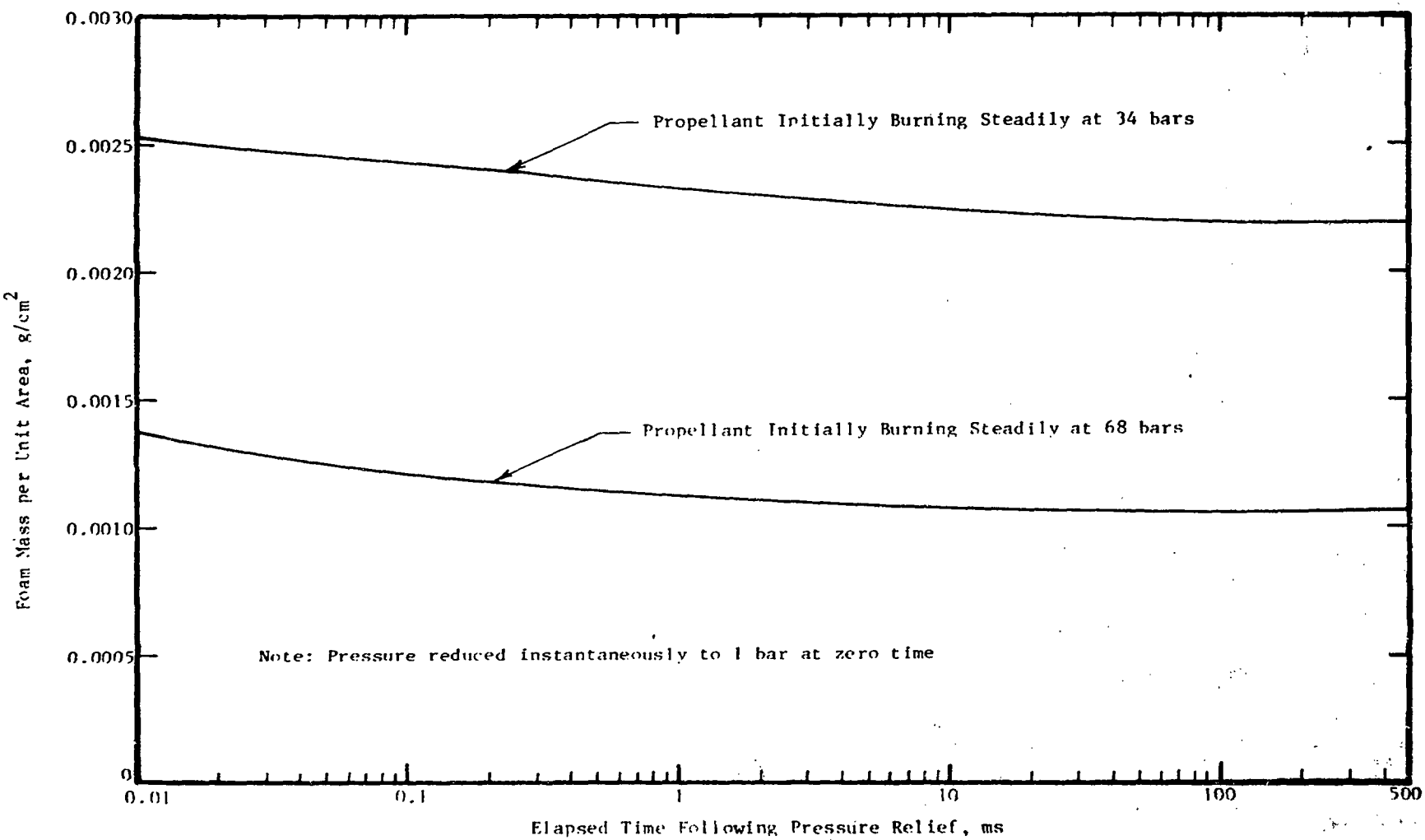

Figure 2. Effect of Pressure Relief Upon HMX Foam Mass

3. CRACK PROPAGATION INTO HIGH PRESSURE/TEMPERATURE GAS CAVITIES

This report considers cracks with a width and length of 0.2 cm and 10.0 cm, respectively. The crack width was chosen sufficiently large to accommodate sufficient hot gas to ignite crack surfaces. The crack length was chosen sufficiently long to afford appreciable differences in the heating of the crack surfaces.

Initially the gases within the crack are considered to be in a state of rest at a temperature and pressure of 294 K and 1 bar, respectively. At zero time the crack is considered to propagate into a cavity of gases whose temperature is 3000 K. Gas pressures within the cavity were varied. The downstream end of the crack is considered either closed, or open to a second cavity containing gases at the same pressure and temperature as those initially within the crack. All gases are assumed to have the same composition.

3.1 Effect of Erosive Heating Upon Steady Burning Conditions

This section is concerned with assessing the effect of erosive heating within cracks upon steady burning of HMX. Table 2 is presented for reference purposes. It gives predicted HMX steady heat fluxes $\bar{q}_f$, burn rates $\bar{r}_f$, foam masses $\bar{M}_f$ and foam temperatures $\bar{T}_f$ as a function of gas pressure P when erosive heating is absent. Figures 3, 4 and 5 indicate the effects of erosive heating upon steady burn rates, foam masses and foam temperatures as functions of the cross-flow gas velocity u for three different pressures, namely 1, 10 and 100 bars. The gas temperature is held constant at 3000 K, while the u value encompasses gas velocities likely to be present within cracks.

Figure 3 indicates that erosive heating can increase the HMX regression rate by a factor as large as nine. The result of more rapid burning is decreased foam mass (see Figure 4) and increased foam temperature (see Figure 5). Of greatest important to the DDT problem are the reductions of foam masses shown in Figure 4 with increased gas velocities u. It may be observed that steady erosive heating can reduce the steady foam mass by as much as an order of magnitude.

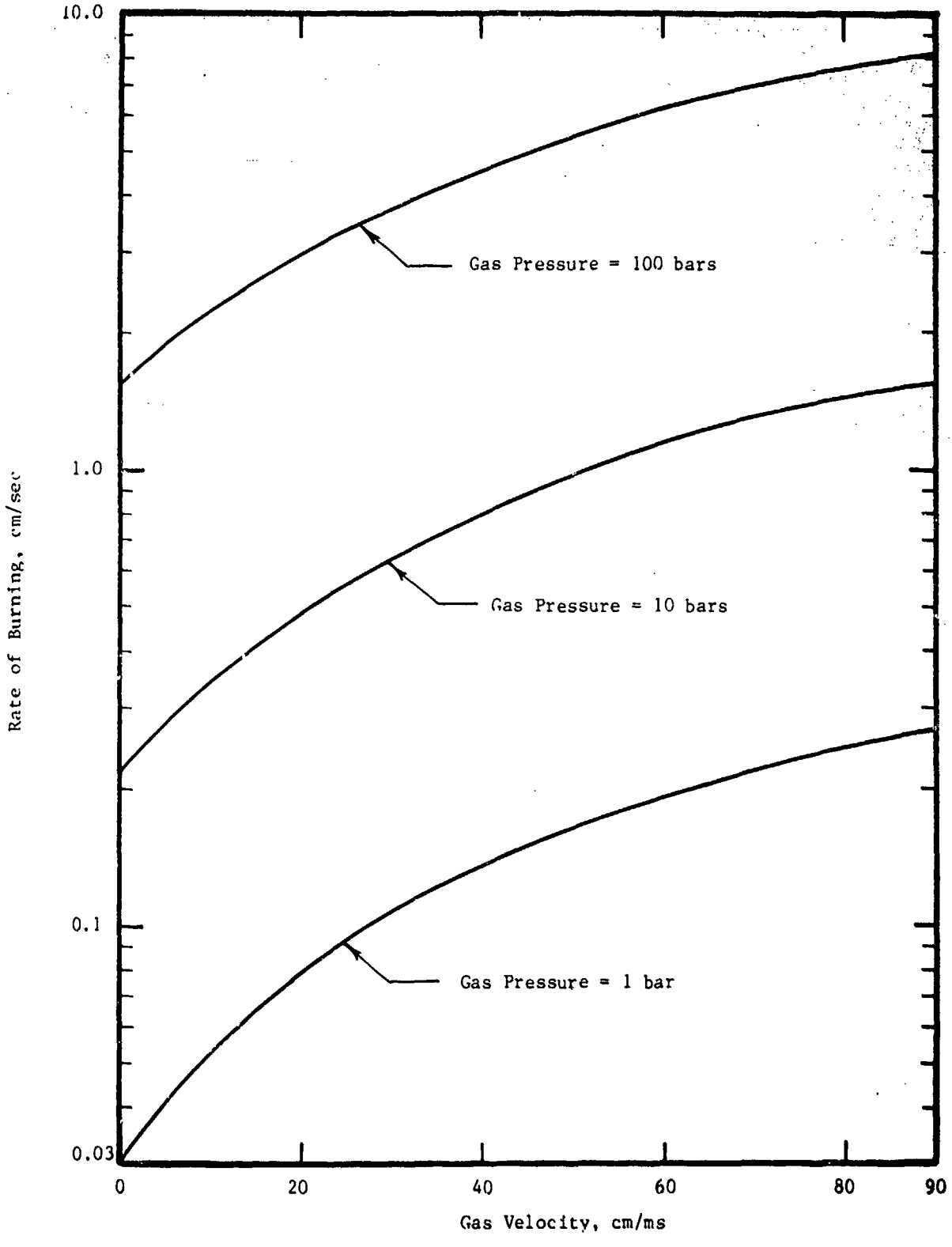

Figure 3. Effect of Erosive Heating Upon Steady Burning Rate of HMX

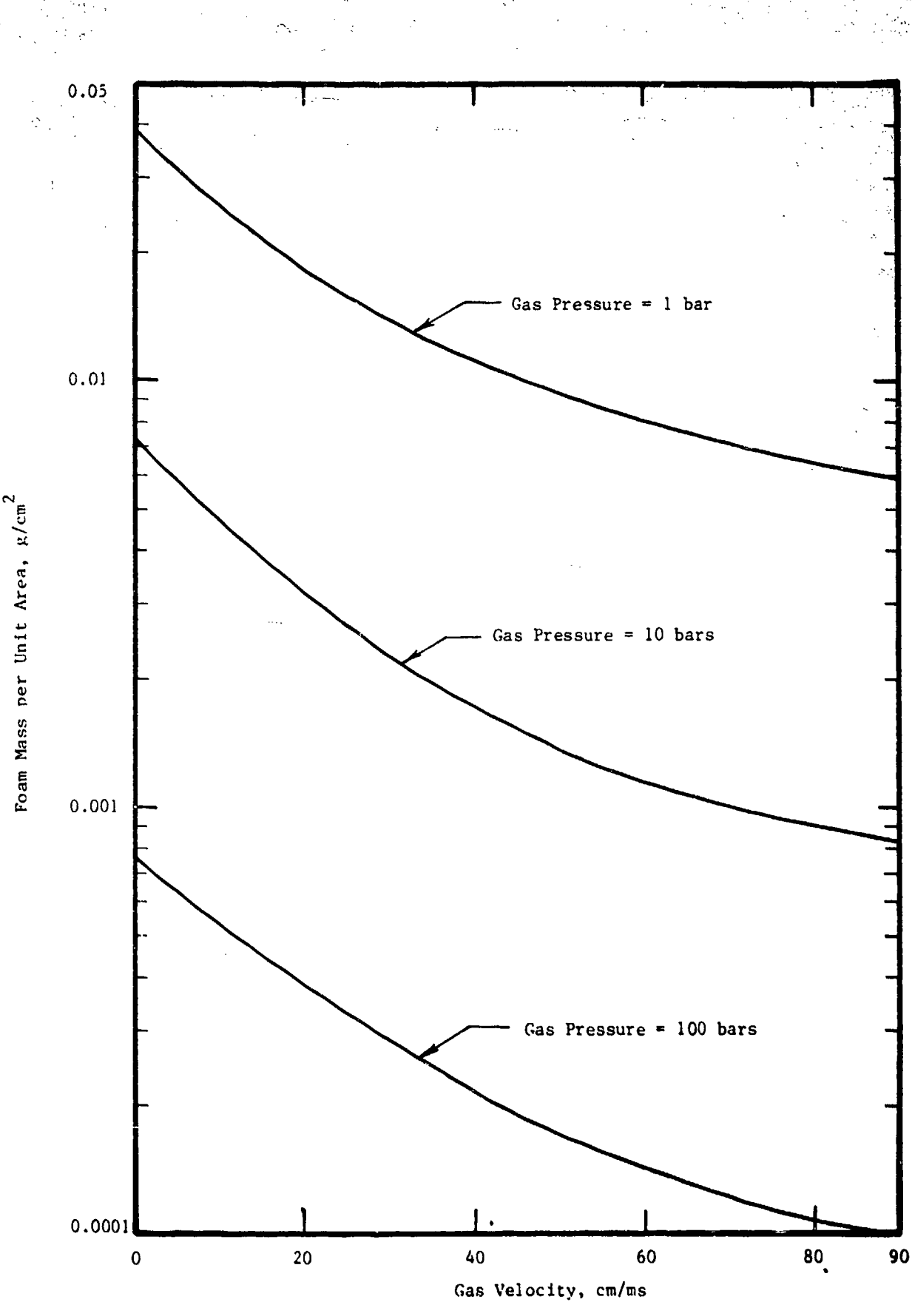

Figure 4. Effect of Erosive Heating Upon HMX Foam Mass During Steady Burning

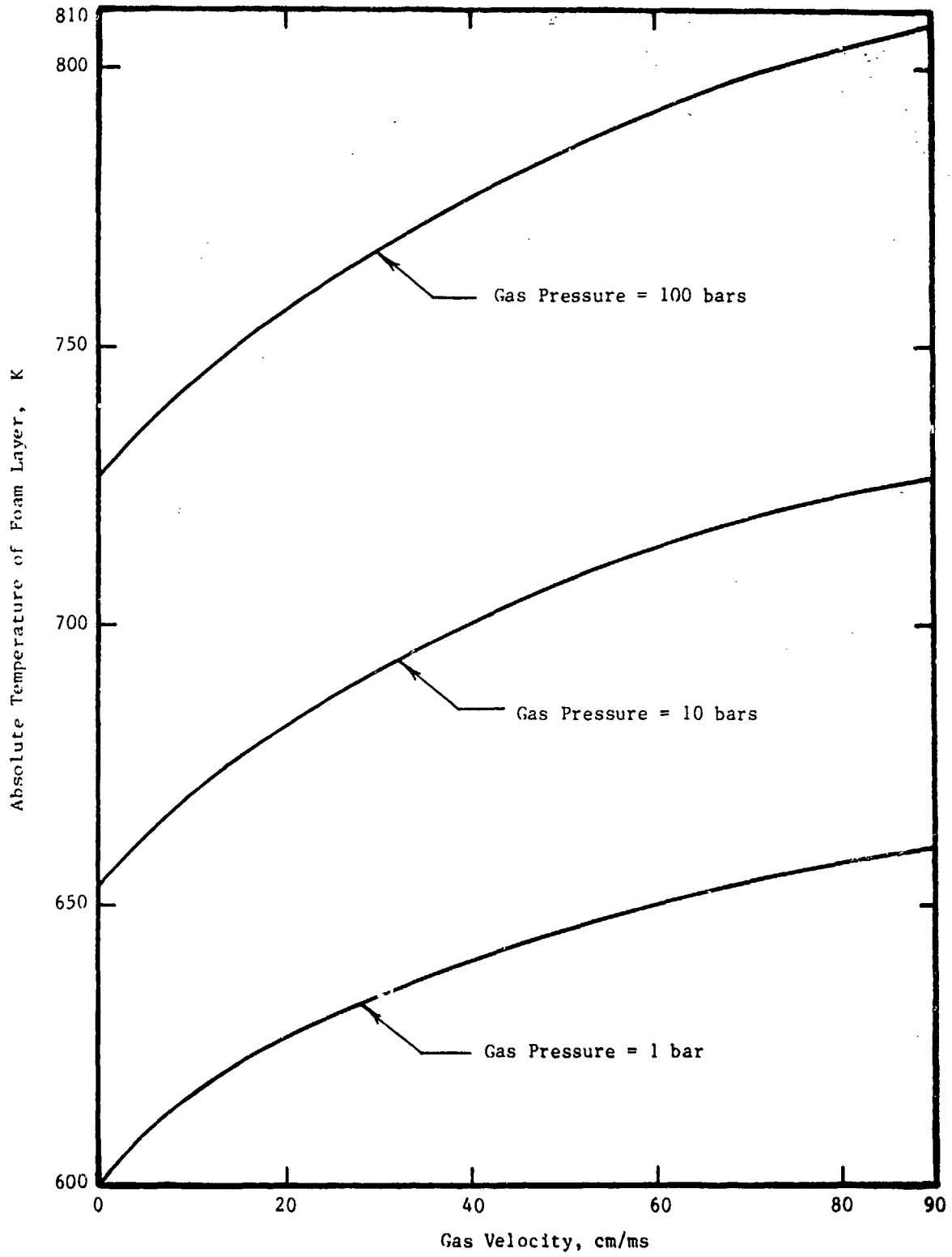

Figure 5. Effect of Erosive Heating Upon HMX Foam Temperature During Steady Burning

TABLE 2. STEADY HEAT FLUXES ($\bar{q}_f$), BURN RATES ($\bar{r}_f$), FOAM MASSES ($\bar{M}_f$), AND FOAM TEMPERATURES ($\bar{T}_f$) DURING HMX BURNING VERSUS PRESSURE (P)

P, Bars	$\bar{q}_f$, cal/cm^2-sec	$\bar{r}_f$, cm/sec	$\bar{M}_f$, g/cm^2	$\bar{T}_f$, K
1	10.0	0.030	0.0367	601
2	19.0	0.055	0.0247	615
5	44.0	0.120	0.0132	635
10	84.0	0.217	0.0075	653
20	160.0	0.394	0.0039	673
30	233.0	0.559	0.0027	686
40	305.0	0.716	0.0021	695
50	376.0	0.867	0.0016	702
60	446.0	1.010	0.0014	709
70	515.0	1.160	0.0012	714
80	583.0	1.300	0.0010	719
90	652.0	1.440	0.0009	723
100	719.0	1.530	0.0008	727

3.2 Depths of Propellant Ignited in "Closed Cracks"

"Closed" refers to cracks whose downstream end is closed. In such cracks, gases will ultimately stagnate in the absence of burning.

Figure 6 presents the maximum depths of propellant ignited within HMX cracks as a function of the cavity pressure. Depths are measured from the upstream end of the crack that is connected to the high-pressure cavity. Times at which the propellant at the maximum depths ignites are presented at the top of Figure 6.

As one would expect, the maximum depth of propellant ignited by the inflow of hot gases increases with the cavity pressure. Ignition times range from a few milliseconds with low cavity pressures, to a fraction of a millisecond with high cavity pressures. The maximum amount of foam generated by the inflow of hot gases occurred with the lowest cavity pressure considered, namely 9 bars. It was only 6.10^{-4} g/cm^2 which is roughly an order of magnitude less than those presented in the next section

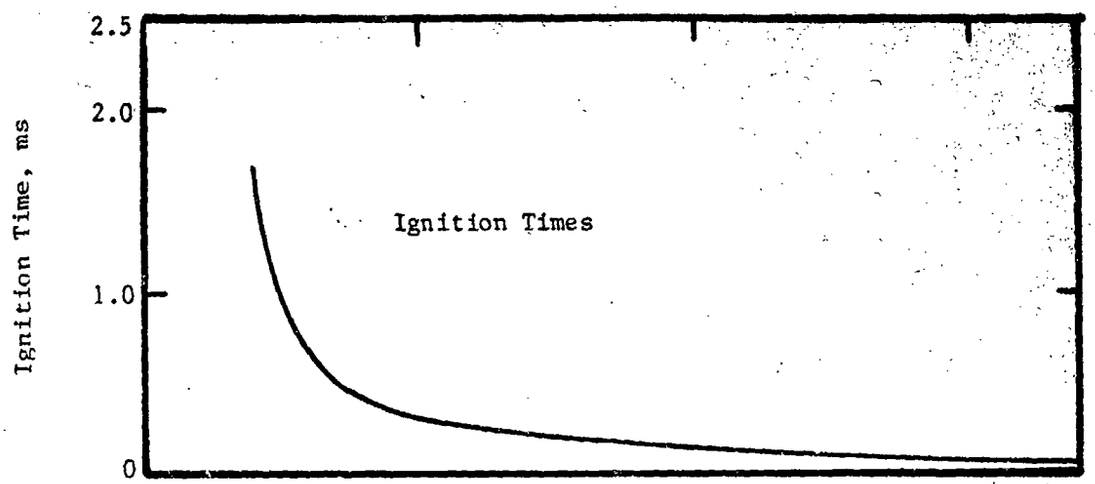

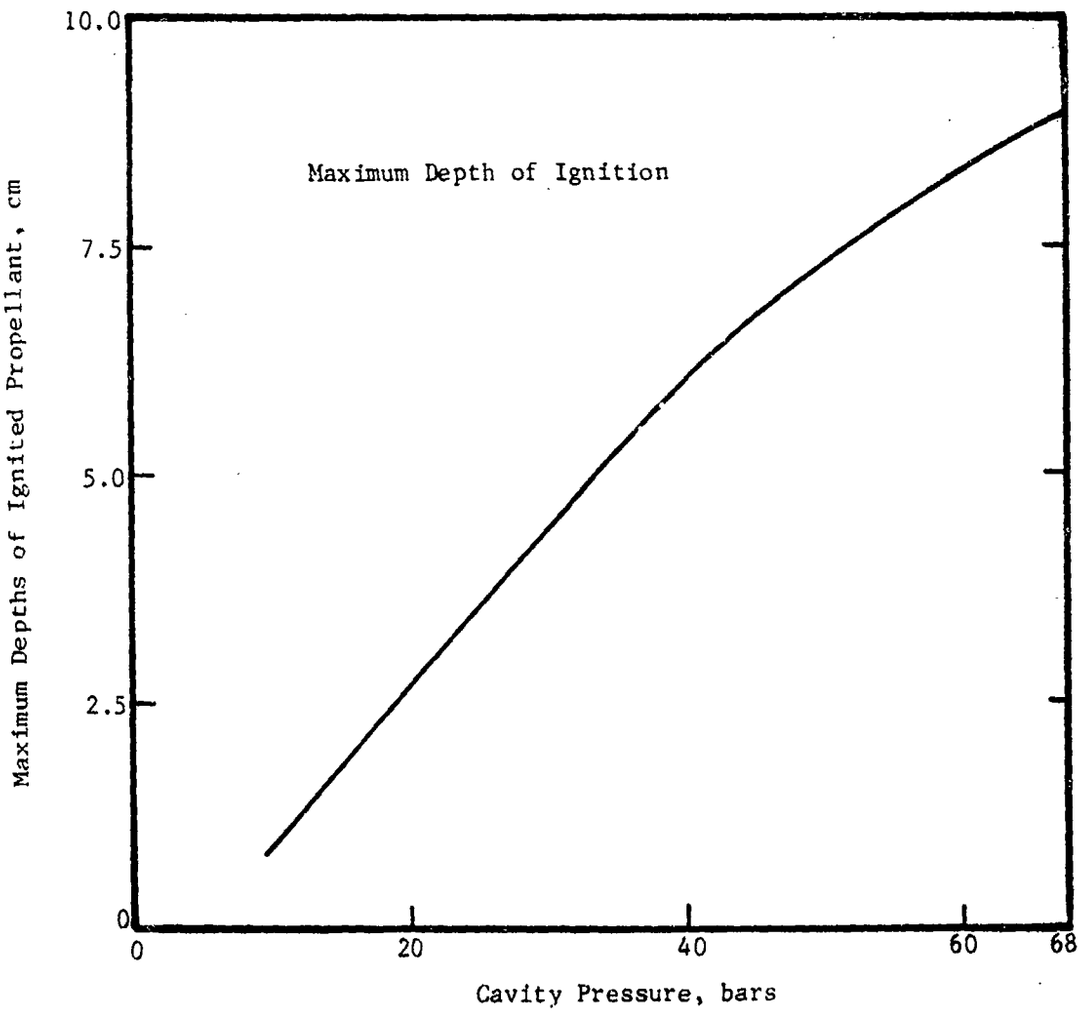

Figure 6. Depths of HMX Ignited in "Closed Cracks" by Influx of Hot Gas

for "open cracks" exposed to the same cavity pressure. This result suggests that closed cracks are not apt to generate appreciable foam unless they are:

(1) Sufficiently long, or wide at their downstream end to prevent pronounced decreases of the heat flux while appreciable foam is being generated, and/or are able to

(2) maintain relatively low gas pressures for sufficient time until near steady-state foam masses are achieved.

These possibilities will be explored following experimental validation of the analytical predictions.

3.3 Predictions for "Open Cracks"

The downstream end of "open cracks" is connected to a cavity of gas having the same pressure and temperature as the gas initially within the crack. With such cracks, hot gases continue to flow through the crack as long as the cavities remain at different pressures.

Figures 7 through 9 present gas velocities, crack widths, gas pressures and foam masses versus crack depth for cavity pressures of 8, 16 and 68 bars, respectively. The dotted, dashed, and solid curves refer to conditions present at specified times following sudden exposure of the crack to the high-pressure cavity.

Crack widths are greatest at the high-pressure cavity end of the cracks due to longer exposures to elevated gas pressures. Crack expansion will continue at least until stress waves are applied to the cracks.

Initially the foam mass is greatest at the high-pressure cavity end of the crack as one would expect. Thereafter, the greatest foam mass occurs at increasing crack depths. Ultimately the foam mass is greatest at or near the downstream end of the cracks. The latter is due to the fact that the heat fluxes at the downstream end of the crack start out small and then gradually increase. The converse is true at the upstream end of the crack.

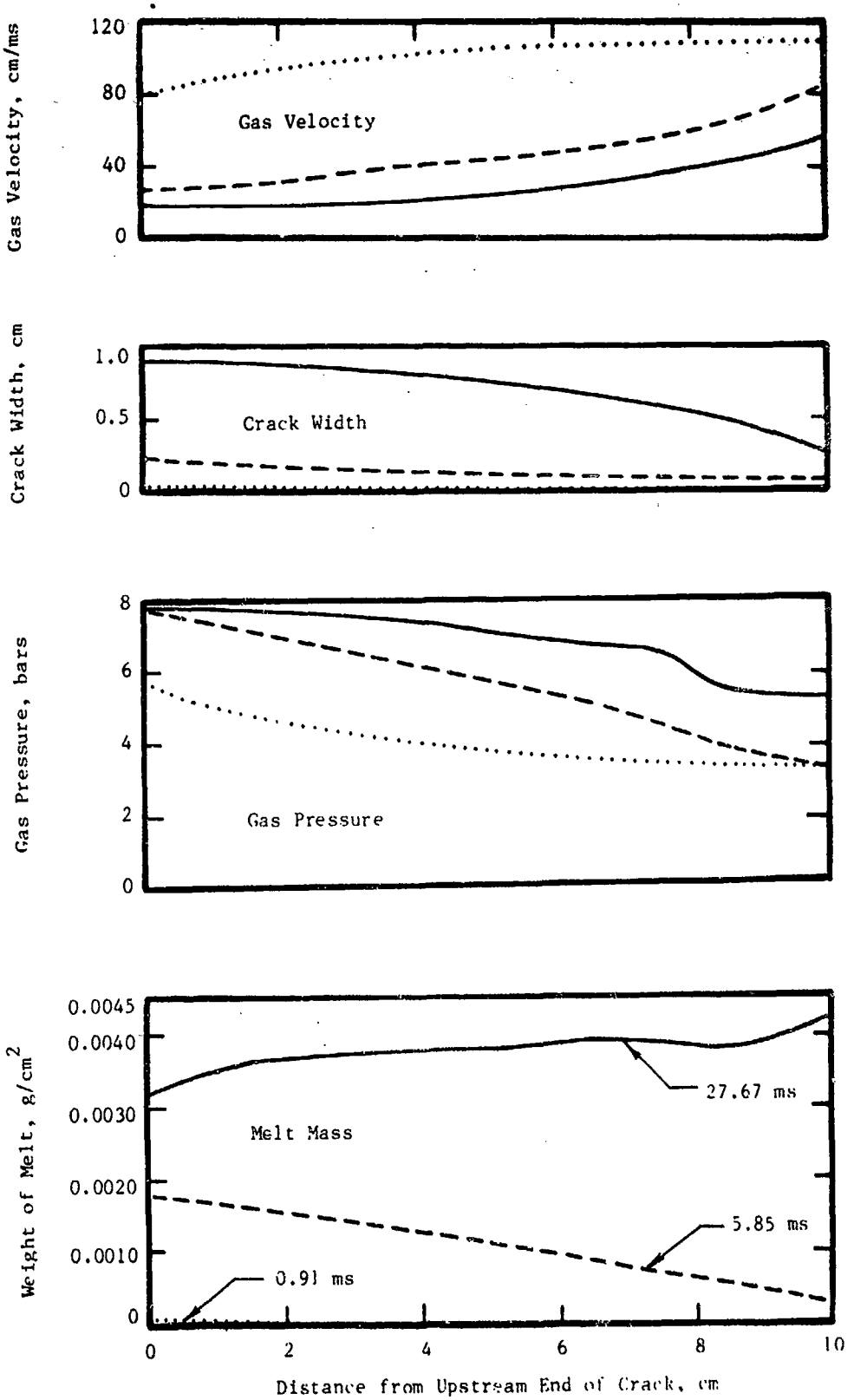

Figure 7. Consequence of Sudden Exposure of "Open Crack" to High Pressure (8 bars) Cavity

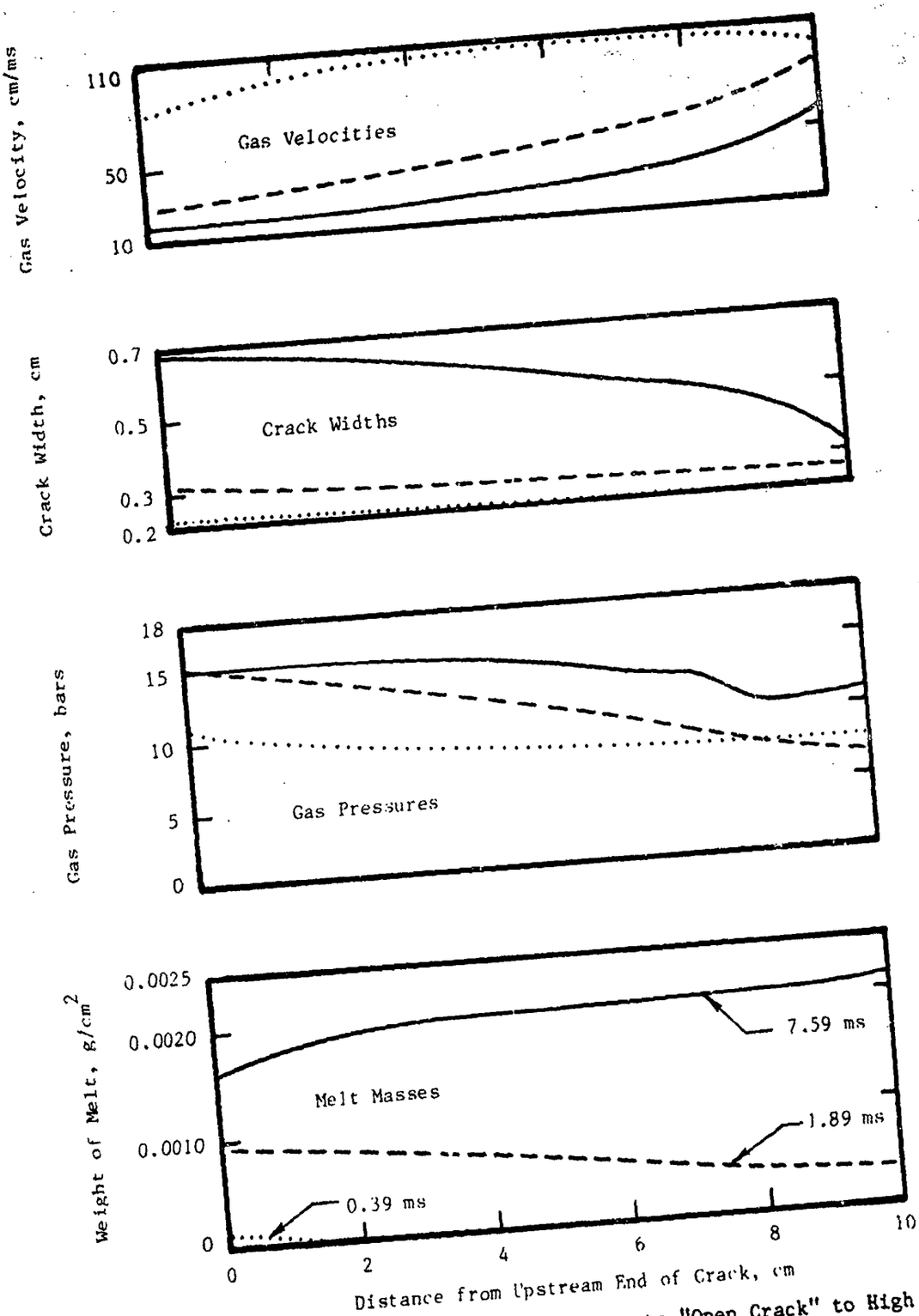

Figure 8. Consequence of Sudden Exposure to "Open Crack" to High Pressure (16 bars) Cavity

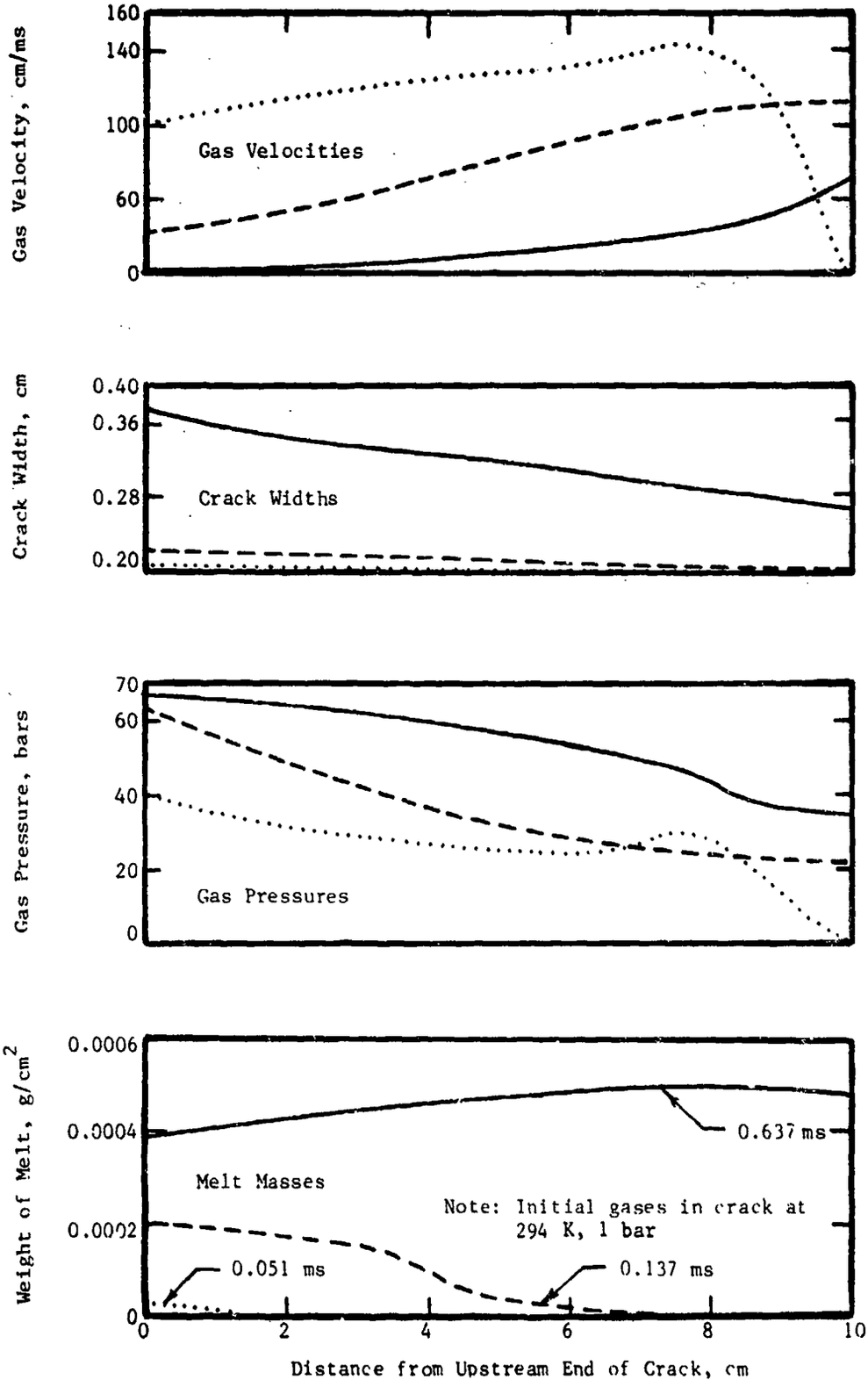

Figure 9. Consequence of Sudden Exposure of "Open Crack" to High Pressure (68 bars) Cavity

Mean values of the foam masses presented in Figures 7 through 9 are shown in Figure 10 as a function of time. The mean value equals the integral of the foam masses with respect to crack depth divided by the total length of the crack. Figure 10 indicates that the mean foam mass asymototically approaches values of about 0.0040, 0.0020, and 0.0005 g/cm^2 for cavity pressures of 8, 16, and 68 bars, respectively. Notice that the above foam masses are roughly inversely proportional to the cavity pressure. The greater the optimal amount of foam is the longer it takes to generate.

At present the masses cited above do not appear adequate to cause DDT unless extremely intense stress waves are generated, say by the presence of multiple burning cracks. Two possibilities exist for foam enhancement. The first is indicated above, namely low gas pressures within the cavity which lessen the rate at which the propellant is heated. The second possibility is the accumulation of melt within cracks brought about by melt flow caused by high velocity gases moving laterally over the foam. The latter possibility remains to be explored. It applies to "closed" as well as "open cracks".

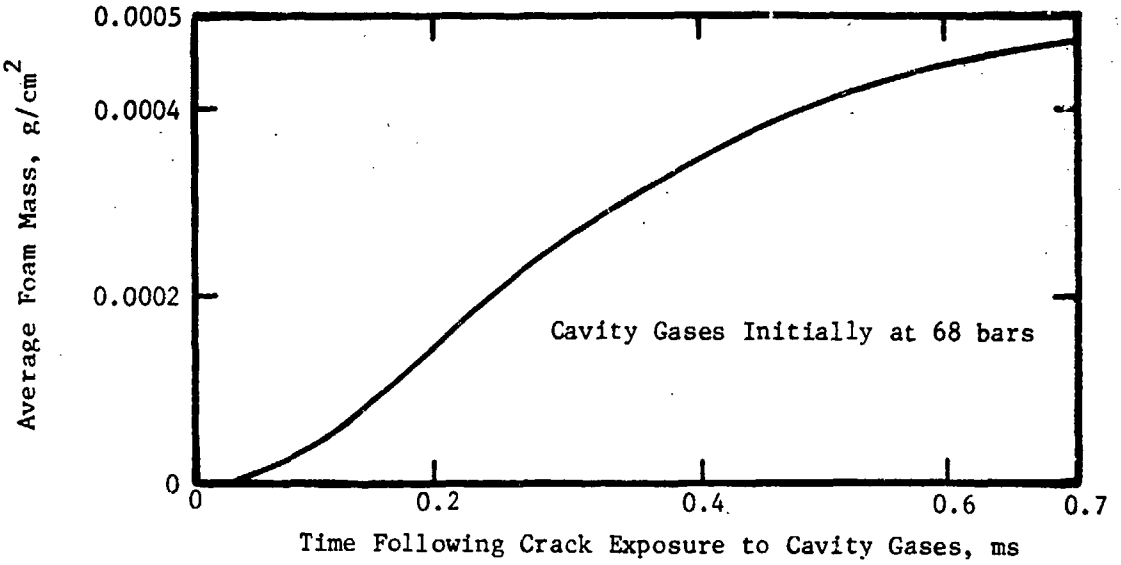

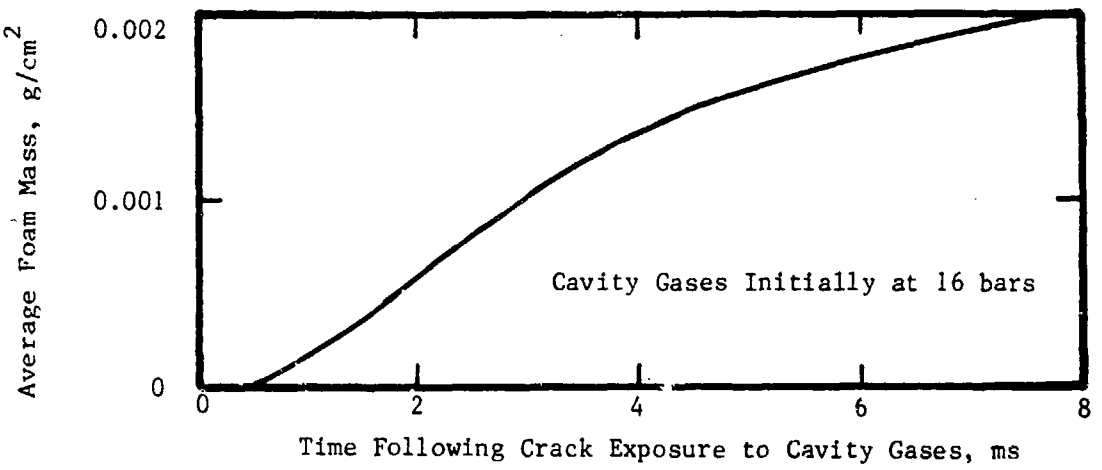

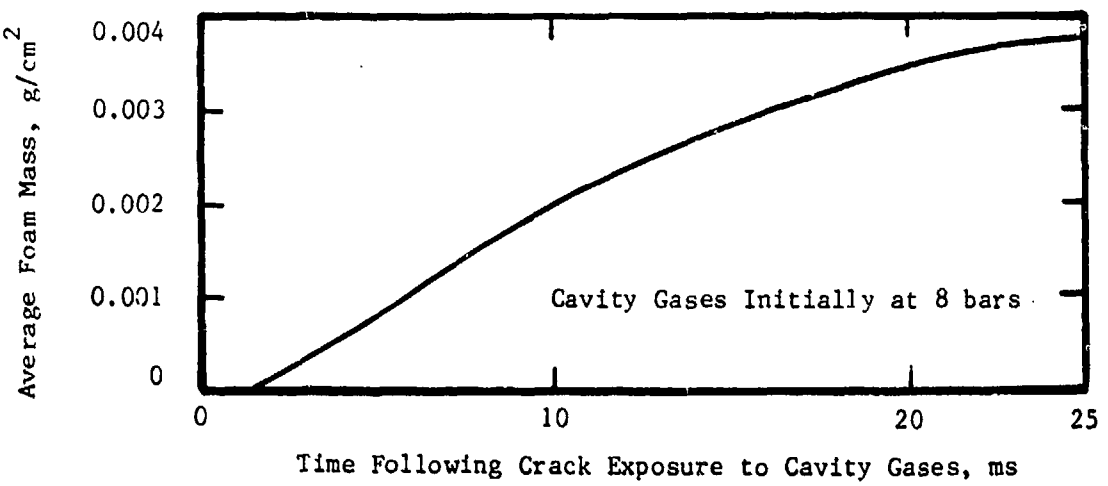

Figure 10. Mean HMX Foam Mass Within "Open Cracks" versus Time

4. EXPERIMENTAL DDT DESIGN

4.1 Design of DDT Apparatus

A preliminary design of a fixture for studying DDT was presented in the previous interim report [4]. Since then the fixture has been revised as shown in Figure 11. The principal difference between the two designs is in the means for heating and igniting the propellant. In the previous design hot nitrogen gas flow was considered as a heat source in order to accentuate melt formation. Hot gas flow will dissipate gases evolved by the heated propellant and increase melt formation by delaying ignition. Ignition may be initiated by turning the nitrogen gas flow off after ignition conditions are achieved.

Since then it was found that the foam mass is extremely dynamic following ignition as shown in Figure 12. The dashed portion of the curve shows how the foam mass increases while it is being heated by an incident heat flux of 1 cal/cm^2-sec. Ignition is assumed to occur when the foam mass achieves a value almost twice that of steady burning.

Figure 12 indicates that the foam mass will rapidly peak and then fall below its steady-state value. Thereafter, the foam mass will oscillate with decreasing amplitudes about its steady value. It may be observed that a time period of only 0.26 sec elapses following ignition before the foam mass decreases to its steady value. Initiating closure of the gas space within such a short time period raises instrumentation difficulties. The first is in the time expended in detecting ignition and in mechanically releasing the driver. These events would require about 0.1 sec. Secondly, a delay of about 0.2 sec would be required before the driver strikes the piston. While one can substantially reduce the free-fall time of the driver, say by the use of compressed gas, it is not warranted at the present time. In this regard, initial tests should be kept as simple as possible until the design functions as anticipated and DDT is achieved.

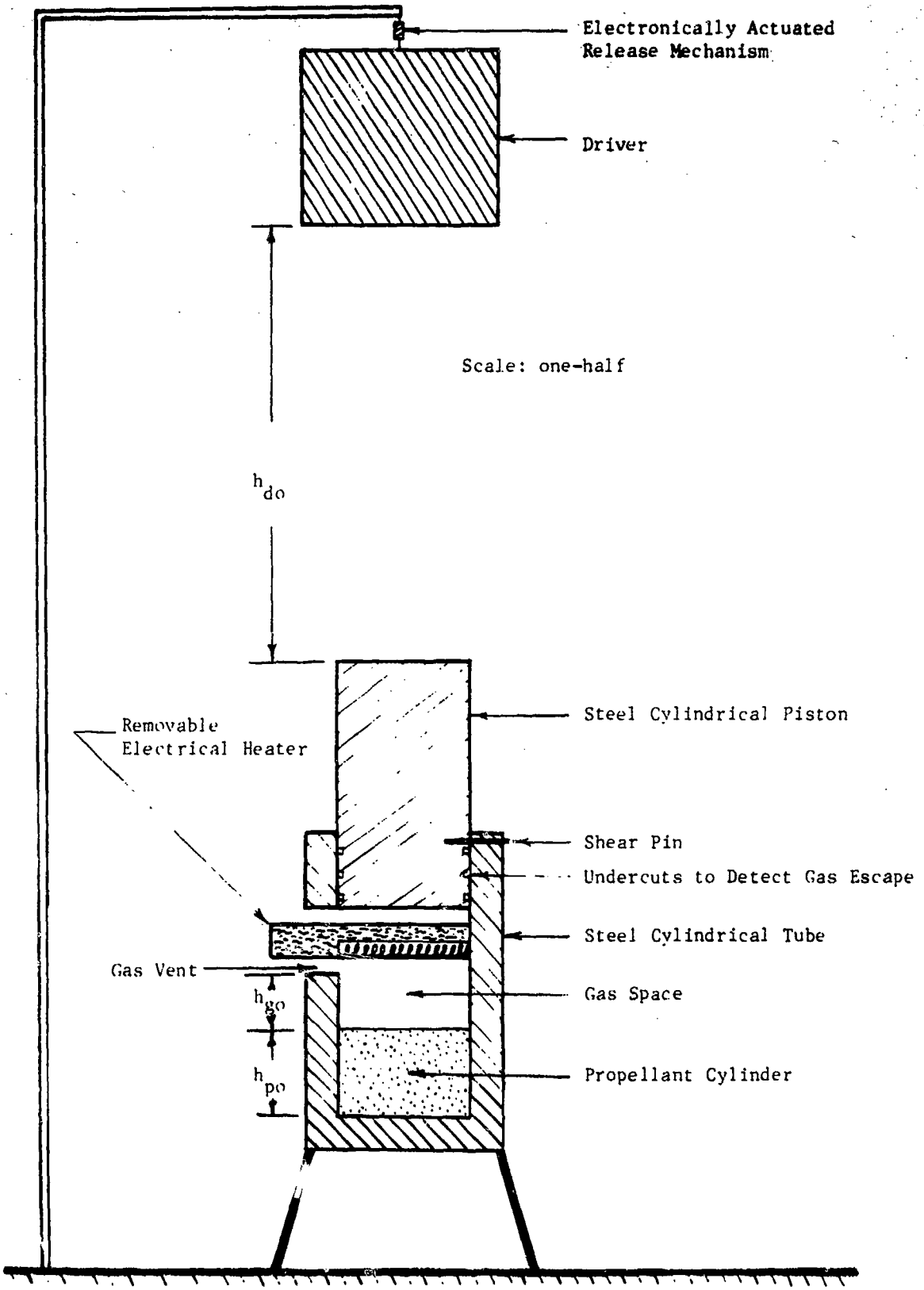

Figure 11. Schematic of Revised DDT Apparatus

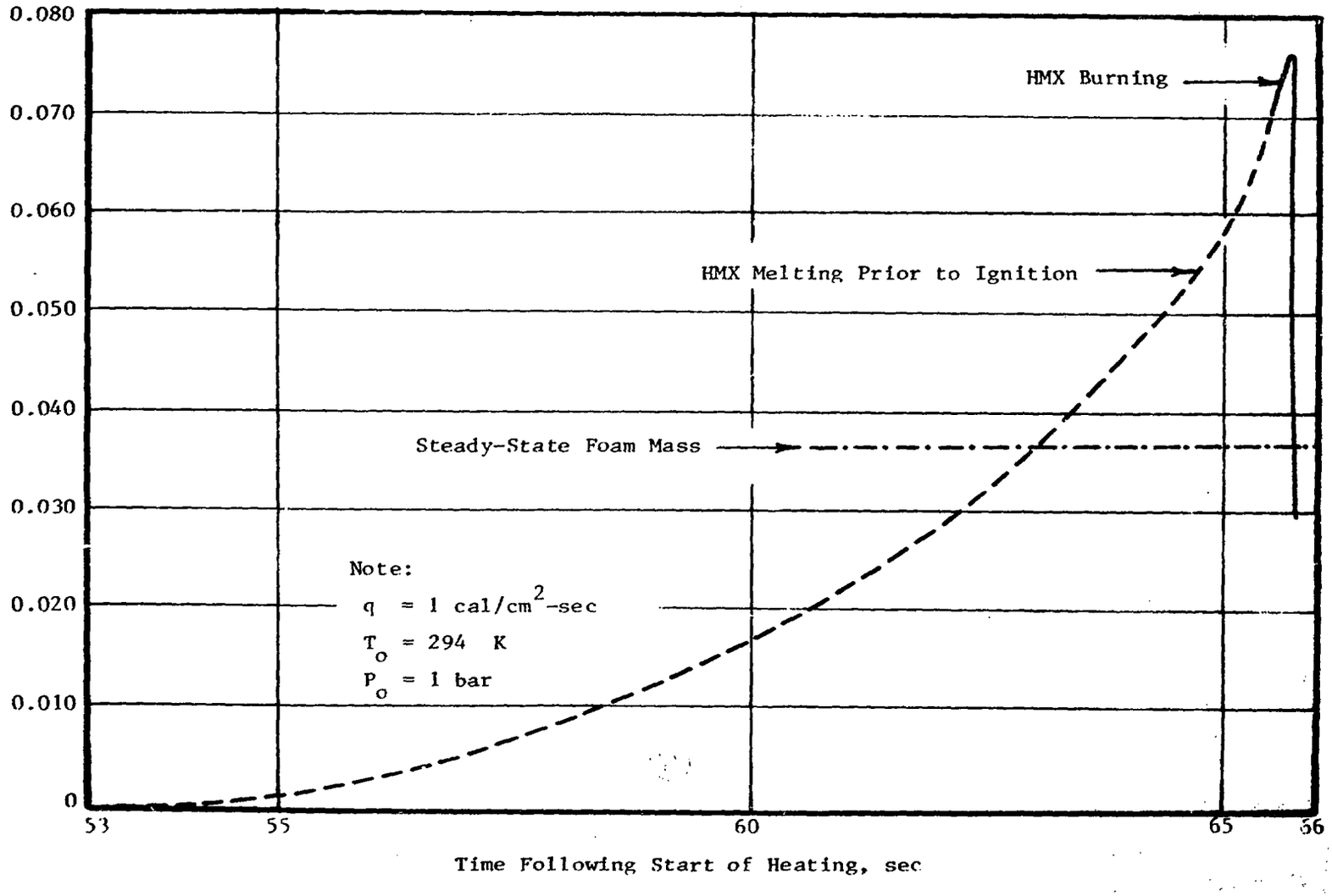

Figure 12. HMX Foam Mass During Melting/Burning

For the above reasons it is planned to burn the propellant steadily before releasing the driver. While steady burning does not provide for optimum foam masses, it has two benefits. The first is consistent burning conditions at the start of closure of the gas space. The second is in being able to use a much simpler heat source, namely the electrical heater illustrated in Figure 11.

Immediately following ignition the heater must be withdrawn and the burning allowed to proceed until steady burning is achieved. Thereafter the driver is released forcing the piston downward. After passing the gas vent the piston will commence to increase the pressure within the gas space. Closure rates may be varied by altering the initial heights h_{do} and h_{go}. By such means it is possible to approximate closure rates of cracks caused by stress waves with amplitudes ranging up to a few hundred bars.

Pressure rises will accentuate propellant heating by increasing the pressure-dependent term of equation (10). The result will be pronounced increases in the rates of burning and pressure rises that will continue to accelerate until the foam is essentially consumed. While gas pressures are rising, stress waves will radiate from the gas space. Following reflection from the steel base beneath the propellant, the stress waves will return and commence to compress the gas space. Transit times of the radiating and reflected stress waves are of the order of 10 μsec. They may be varied by adjusting the height h_{po} of the propellant cylinder.

4.2 Analytical Results

Five factors affect pressure buildup within the gas space. They are:

(1) Initial altitude (h_{do}) of the driver above the piston,

(2) Initial height (h_{go}) of the gas space,

(3) Initial height (h_{po}) of the propellant cylinder,

(4) Initial foam mass (M_{fo}),

(5) Initial foam temperature (T_{fo}), and

(6) Driver mass (W)

The remainder of this section is concerned with the consequence of varying items 1 through 4 individually. Nominal values for the above parameters are presented below:

h_{do} = 1 ft

h_{go} = 2.5 cm

h_{po} = 5.0 cm

M_{fo} = 0.0367 g/cm^2

T_{fo} = 601 K

W = 100 lb

The above combination of parametric values was chosen in that it results in near-optimal pressure rises in the gas space. Values assigned for the mass M_{fo} and temperature T_{fo} are associated with the steady burning of HMX at 1 bar of pressure (see Table 2).

Figure 13 presents predicted gas pressures P and the gas space heights h_g as a function of time until the pressure peaks. Figure 14 presents extremely dynamic portions of the Figure 13 curves on either side of the pressure peak.

Figure 13 indicates the pressure will peak at about 30 kbars in 10 msec following the start of closure of the gas space. Figure 14 suggests that much of the above pressure rise will occur within only a fraction of a μsec. Thereafter the pressure decays in an exponential fashion as a consequence of expansion of the gas space by the pronounced gas pressures.

Results shown in Figures 13 and 14 are predicated on no heat losses from the foam to the piston, and the presence of planar stress waves whose amplitude is not altered in moving through the propellant. There is a distinct possibility of foam-piston contact in that the surface of the burning propellant will become

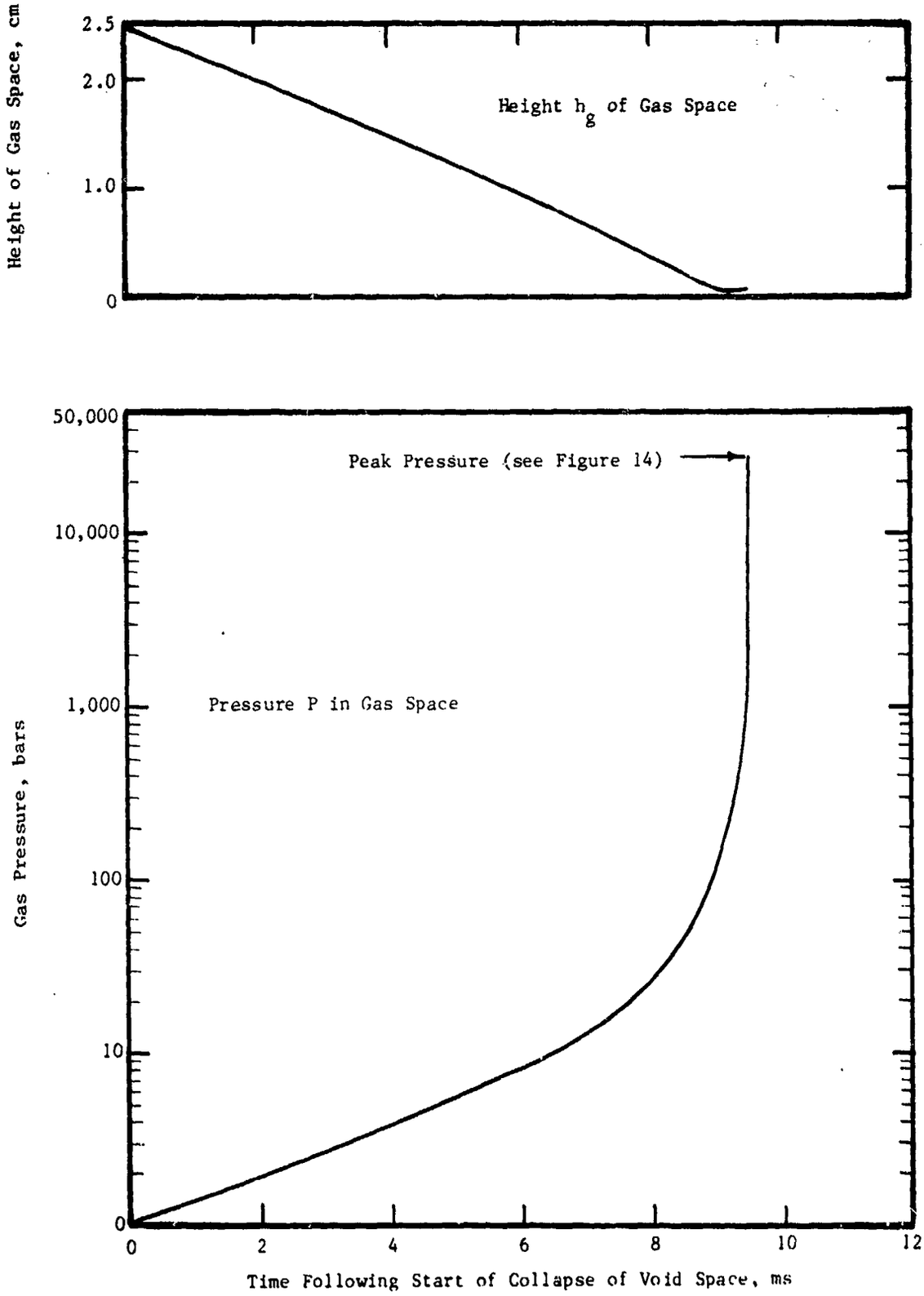

Figure 13. Consequence of Dropping 100-lb Driver from 1 ft

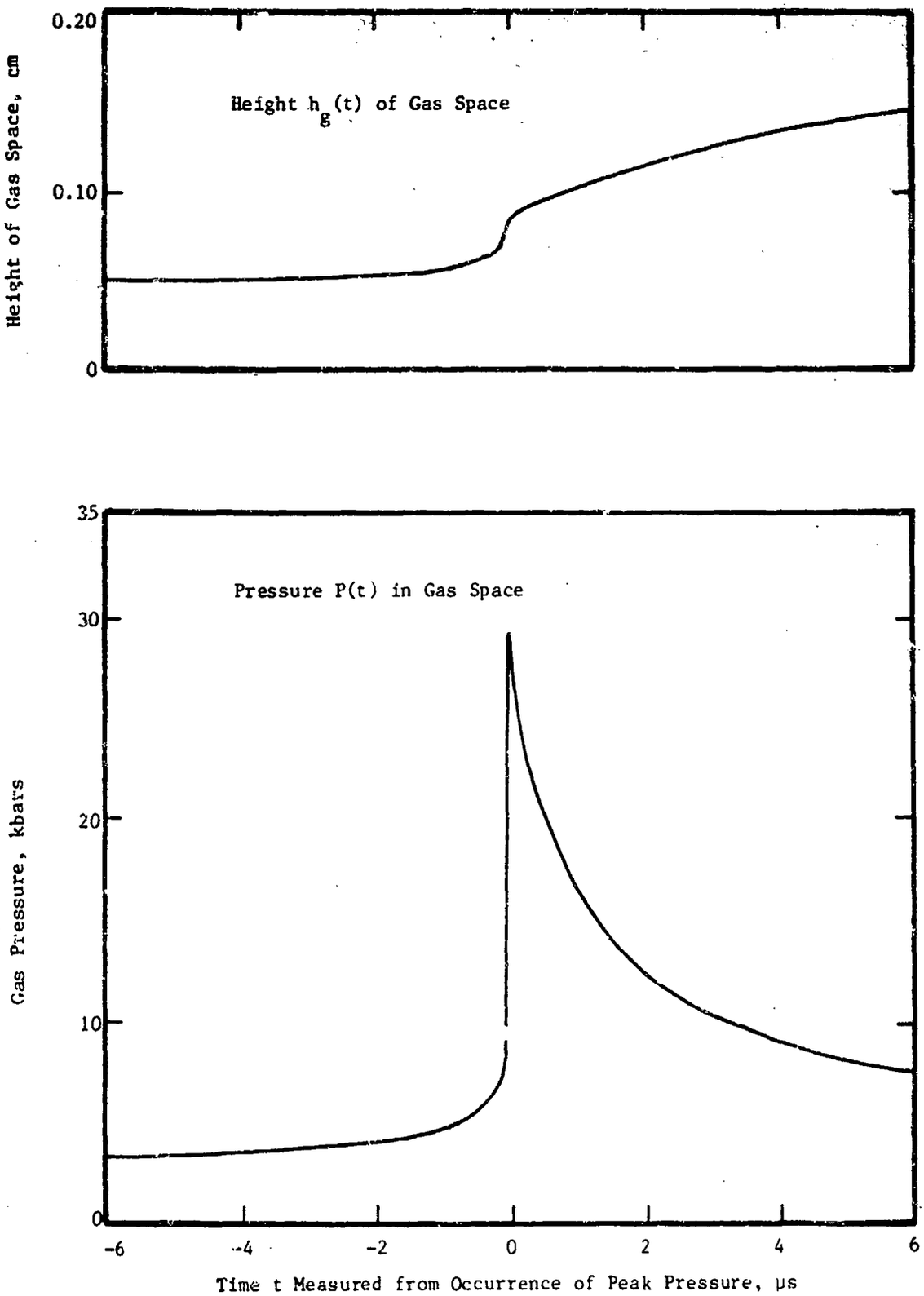

Figure 14. Microviews of Figure 13 Results

concave. Moreover the foam layer is inherently irregular. It is estimated that the foam may be in contact with the piston for as long as 1 ms and thereby lose a significant fraction of its sensible heat. As a consequence the bottom face of the piston should be covered with a thin layer of high temperature insulation. Planar stress waves may be approximated by using propellant cylinders with relatively large cross-sectional areas for the given cylinder length.

Figures 15 through 17 illustrate the consequence of varying the initial values for h_d, h_g, and h_p upon the peak gas pressure and associated void height. Pressure-time curves are not presented in that their shape is very similar to that shown in Figure 14. In the above figures plots of the maximum pressure achieved and corresponding height of the gas space are given as functions of the initial value of the specified parameter under consideration. Remaining parameters are equal to the nominal values cited earlier.

Figure 15 indicates that the driver should be at least 0.5 ft above the piston in order to achieve near optimal gas pressures. Peak pressures do not differ appreciably for driver altitudes between about 0.5 and 2 ft.

Figure 16 indicates that optimal value of the peak pressure will be produced when initial gas space height h_{go} is in the vicinity of 2.5 cm. Above and below 2.5 cm, the pressure decreases monotonically. In this regard smaller heights h_{go} lessen the time period over which the gas space is compressed. The result is lower foam temperatures and hence less dynamic burning. On the other hand, heights h_{go} greater than 2.5 cm increase the gas volume at the time at which the peak pressures occur, and thereby lessen the peak pressure.

Figure 17 illustrates the consequence of varying the initial height h_{po} of the propellant cylinder. It may be observed that decreases in the height of the propellant cylinder accentuate the gas pressures. Increased gas pressures are caused by more rapid reflection and return of stress waves radiated from

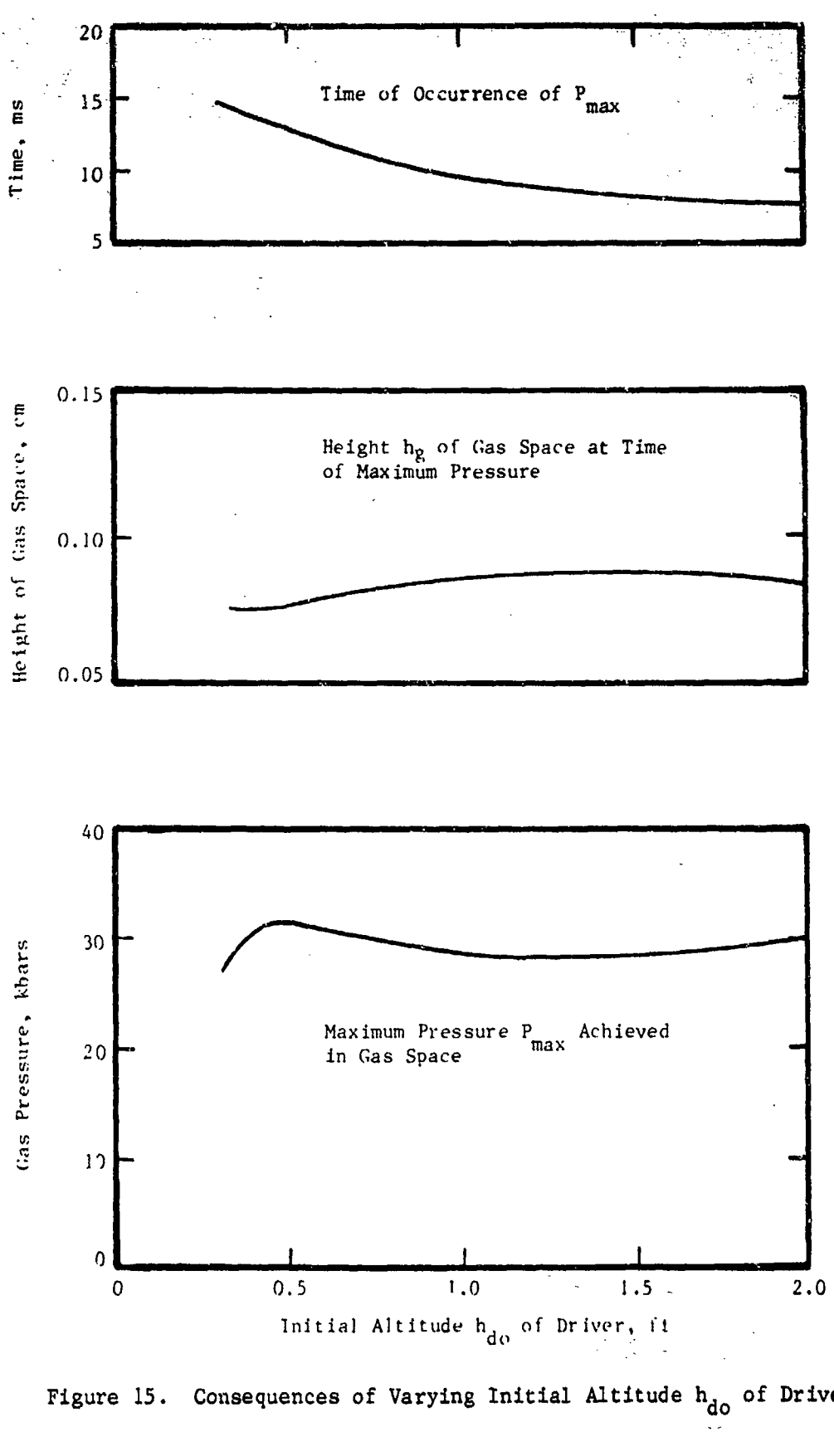

Figure 15. Consequences of Varying Initial Altitude h_{do} of Driver

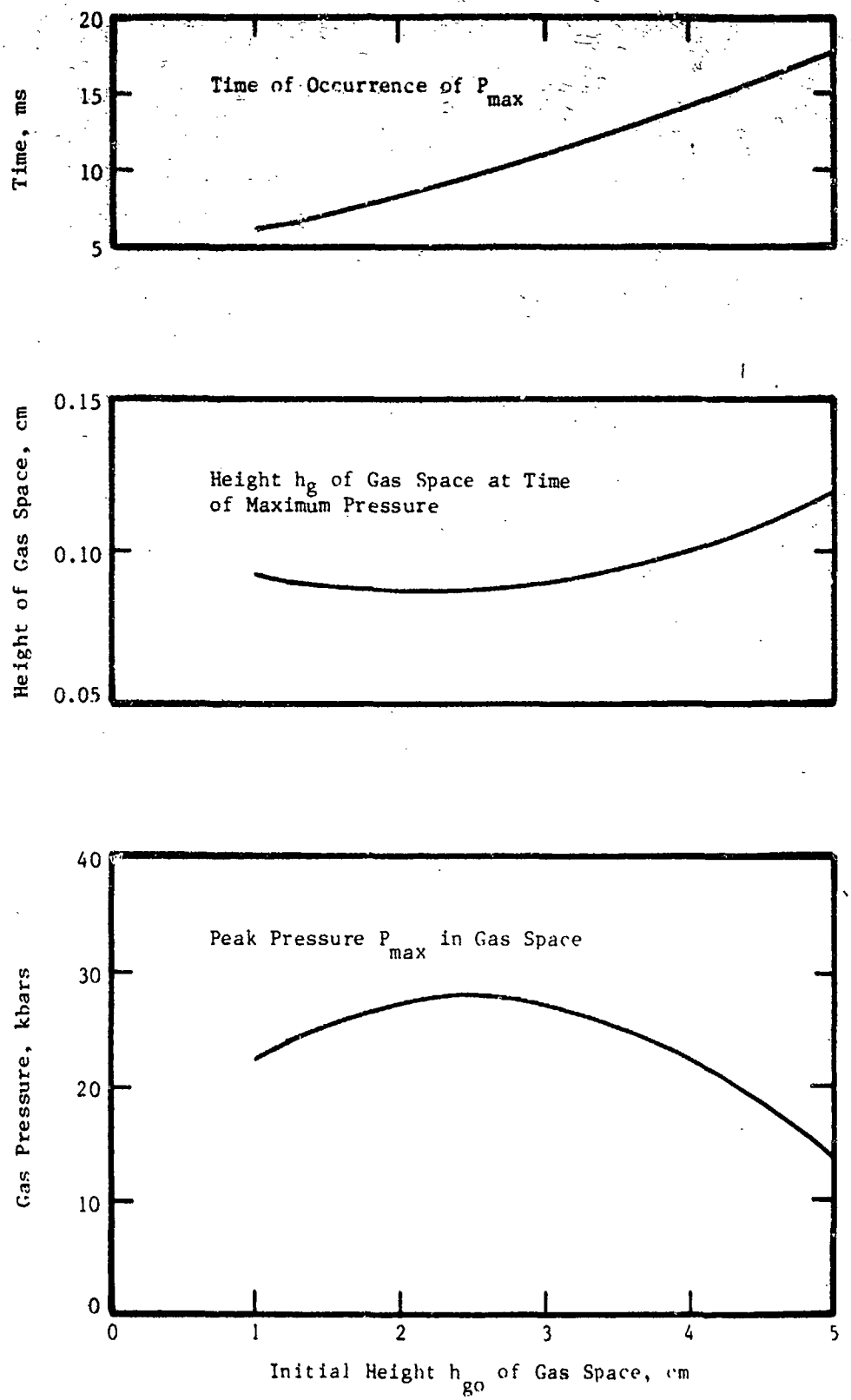

Figure 16. Consequences of Varying Initial Height h_{go} of Gas Space

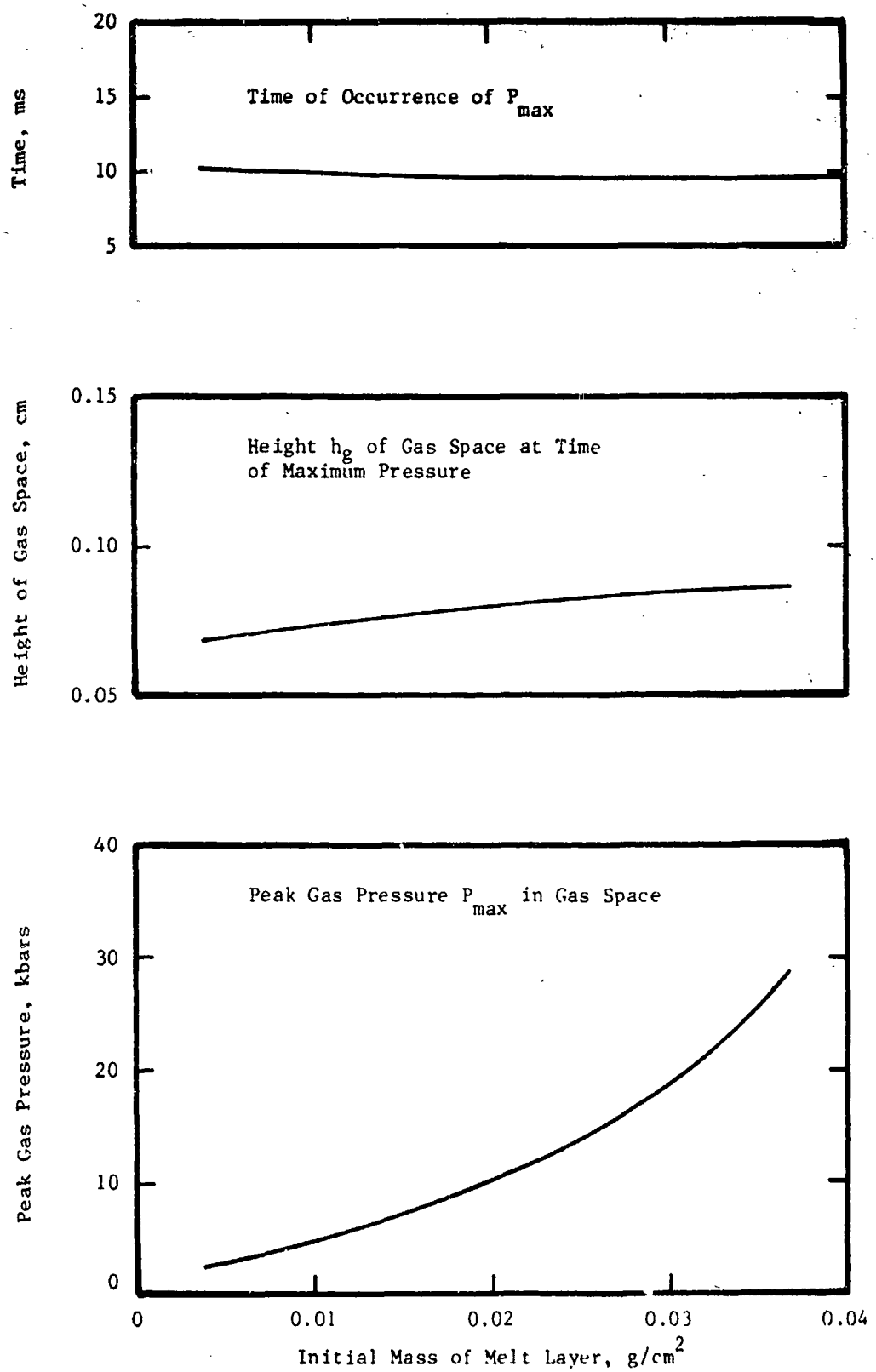

Figure 17. Consequences of Varying Initial Height h_{po} of HMX Cylinder

the gas space. The result is higher amplitude stress waves being applied to the gas space at least during periods of rising pressure.

Figure 18 shows the effect of varying the initial foam mass M_f. It may be observed that the peak pressure is highly dependent upon the foam mass. That is why we are so concerned with the generation, and possible transport and accumulation of melt within cracks.

Finally it is important to know how well the initial temperature of the propellant needs to be controlled to achieve consistent test results. Of concern is the sensitivity of the steady burn rate, and mass and temperature of the foam mass to the initial temperature of the propellant. Figure 19 illustrates the above dependence. Notice that the foam mass is optimal with initial propellant temperatures between about 270 and 320 K. High initial temperatures accentuate the burn rate as well as the foam temperature. For purposes of test consistency, the initial temperature of the propellant should be maintained within about $\pm$20 K of the normal room temperature of 294 K. Only during very cold days will temperature control be needed.

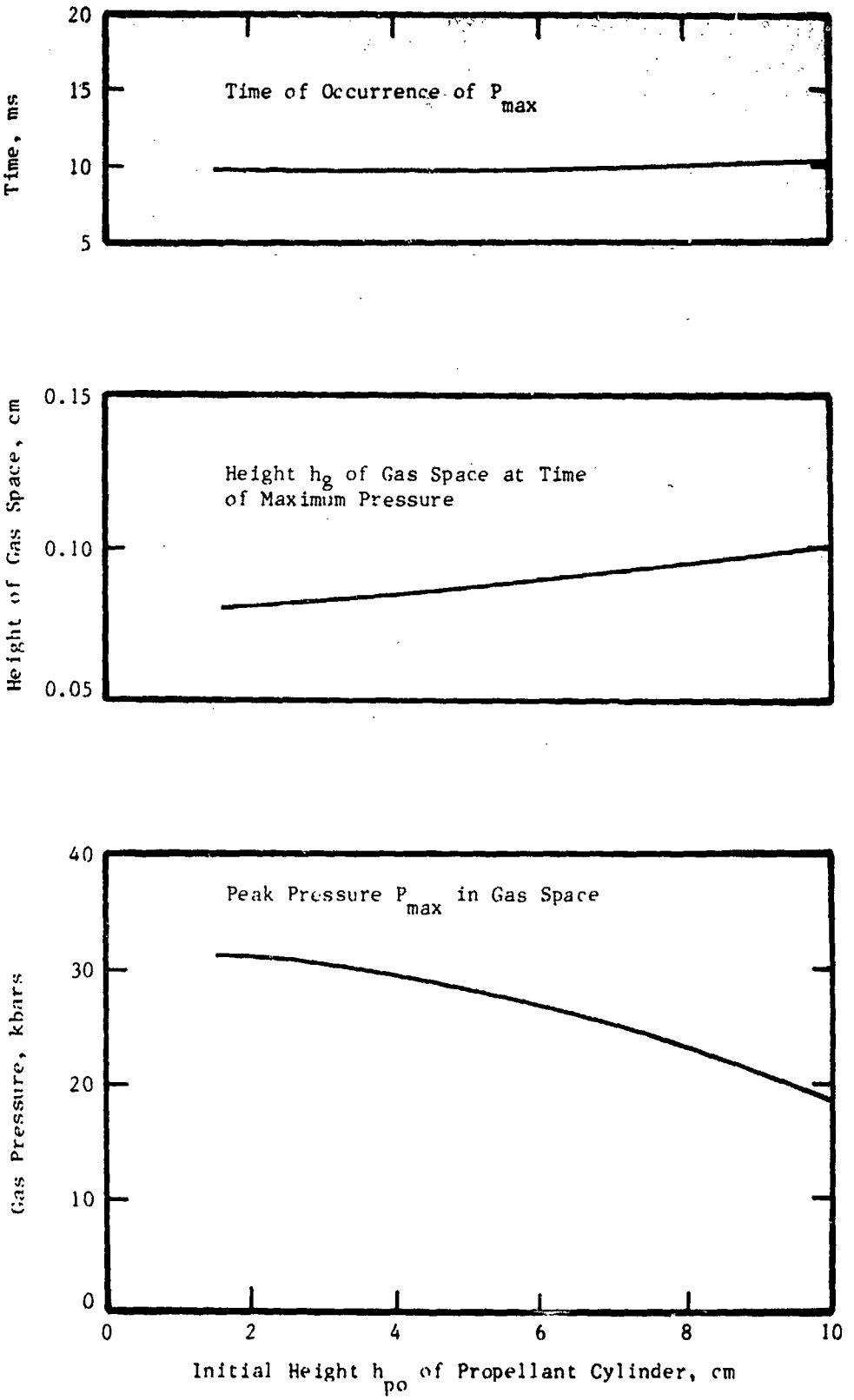

Figure 18. Consequences of Varying Initial Mass M_{fo} of HMX Foam Layer

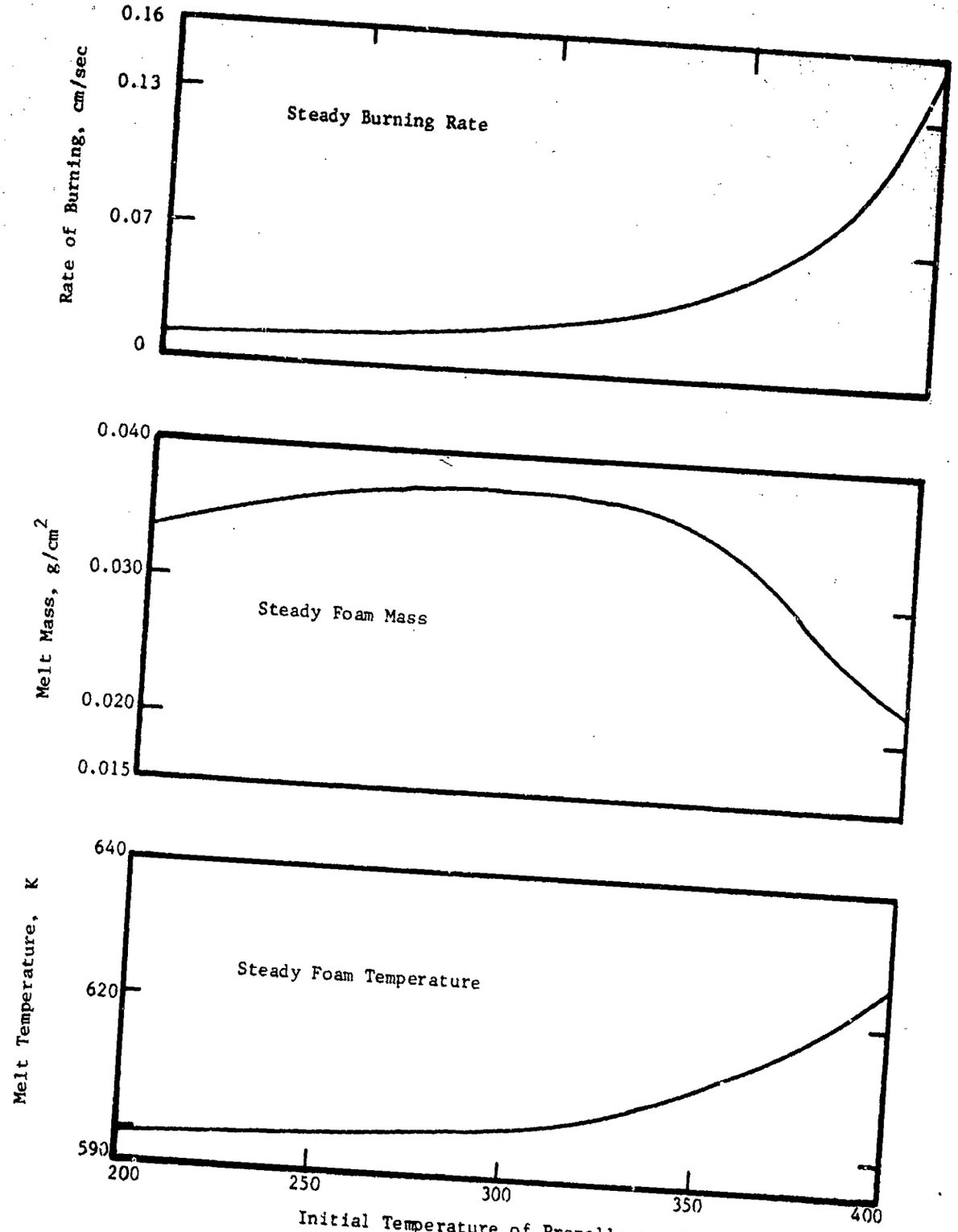

Figure 19. Effect of Initial Temperature of HMX Upon Steady Burning Conditions

5. SUMMARY, CONCLUSIONS, AND FUTURE PLANS

5.1 Crack Studies

These studies were concerned with assessing the consequence of crack propagation into cavities containing gases at higher pressures and temperatures than initially exist within the cracks. The result of this and previous studies [2-4] reveal three important factors in causing DDT. They are the presence of:

(1) appreciable amounts of foam or melt,

(2) high temperature foam, and

(3) high amplitude stress waves.

Item 1 is important in that much of the foam is consumed during accelerated burning. The latter includes the foam present at the start of the pressure transient plus additional foam generated by melting during the pressure transient. Usually the added foam is a small fraction of that present at the start of the pressure transient.

Item 2 is important in that high foam temperatures speed foam consumption and thereby decrease the time over which cracks are expanded by elevated gas pressures. The importance of item 3 lies in the fact that high amplitude stress waves not only trigger accelerated burning but also retard crack expansion. In this regard, gas pressures always peak while cracks are expanding rather than contracting.

Analytical studies reveal that single burning cracks are more likely to cause DDT when they are in close proximity to the motor case. Close proximity leads to more rapid reflection and return of stress waves radiating from the crack. The result is more intense stress waves being applied to the crack at least during periods of rising pressure. In turn, high amplitude stress waves accentuate gas pressures within the cracks by speeding the burning and restricting crack expansion.

The above DDT possibility involves only a single crack. It is in addition to the DDT possibility advanced earlier [4] for situations in which multiple burning cracks are present. In the latter situations, stress waves can be progressively amplified in moving from one crack to the next crack and thereby progressively enhance gas pressures produced within the cracks.

Several propellant properties affect the pressure transients produced in burning cracks. The first is the heat transfer coefficient associated with the transfer of heat from the foam to the solid propellant interface. Greater heat transfer coefficients increase foam buildup. Of equal importance are the propellants activation energy and internal heat constant. In this regard, large activation energies or internal heats act to accelerate the burning.

At present we are primarily concerned with phenomena affecting foam generation within cracks. For this purpose we have examined the generation of foam within cracks that propagate into cavities containing gases at much higher temperatures and pressures than initially exist within the cracks. The downstream end of the cracks was considered connected to a low pressure cavity so that gases continued to flow through the crack. Not surprisingly, foam masses decreased with increased pressures within the cavity at the upstream end of the crack. Thus, cavity pressures of 8, 16 and 68 bars yielded average foam masses of approximately 0.004, 0.002, and 0.0005 g/cm^2, respectively. Notice that the above foam masses are roughly inversely proportional to the cavity pressure.

In the previous interim report [4] it was shown that pressures of the order of tens of kbars may be generated within multiple burning cracks contained 0.005, 0.010, and 0.015 g/cm^2 of foam. Less cracks are needed to develop such pressures the greater the amount of foam present. Most of the pressure rise occurred within 1 μsec or less.

5.2 Peripheral Studies

Additional studies involved predicting the ignition of HMX, errors in estimating foam masses by pressure relief quenching of the burning, and the consequence of erosive heating upon foam masses.

Cursory examination of HMX ignition suggests that foam temperature presents a satisfactory criterion for predicting ignition. Analysis indicates that the ignition time of HMX is inversely proportional to the square of the incident heat flux. Results remain to be confirmed experimentally.

Pressure relief has a small but significant effect upon HMX foam mass while it undergoes solidification. Analysis indicated that the foam mass is reduced by 13 and 19 percent during pressure relief extinguishment of steady burning at 34 and 68 bars, respectively.

Erosive heating is due to the interaction of gases leaving a propellant with gases flowing laterally through a crack. It was found that erosive heating very appreciably reduces the generation of foam. HMX foam masses can be decreased by as much as one-tenth of their normal burning (no lateral gas flow) values depending upon the rates of mass transport by the two gas flows.

5.3 Analysis of Experimental DDT Design

An experimental fixture for studying DDT was described (see Figure 11). Assessments were made of the influence of various fixture parameters upon pressure transients produced by compressing the gas space over burning HMX. It was found that pressure rises of the order of a few tens of kbars may be generated within fractions of 1 μsec. DDT appears likely with such rapid and pronounced pressure buildups [15].

5.4 Future Plans/Needs

During the forthcoming year it is planned to:

(1) conduct the DDT experiments described in Section 4 using a composite propellant consisting of 65 percent HMX and 35 percent polyethyleneglycol

(2) analyze possibilities by which melt may accumulate within cracks due to possible displacement of the melt by gases flowing along the length of the crack

(3) measure foam masses produced by steady burning of HMX and/or the composite propellant described by item 1 at 1 atmosphere of pressure.

The initial DDT experiments (item 1) are primarily concerned with establishing whether or not DDT occurs. Expensive pressure transducers shall be reserved for follow-on experiments if DDT occurs. Item 2 involves development of a subroutine for the computerized model PROS described in sections 1 and 2. Item 3 is important in establishing whether or not extrapolated HMX foam masses used in this report are reasonable. This comparison is also needed in that the heat transfer coefficient associated with heat flow from the foam to the melt interface was deduced from the pressure dependent foam mass present during steady burning.

Follow-on plans will, of course, depend upon information gathered from the above activities. At a minimum they should include:

- upgrading DDT experimental fixture (see Figure 11) to provide for variations of the initial foam mass. This may be achieved by controlling the size of the gas vent and hence the pressure in which the propellant burns steadily prior to releasing the driver.
- conducting DDT experiments with various composite propellants containing HMX
- using analysis and experimental results to identify compositions and critical property values of composite propellants that should be avoided to minimize the likelihood of DDT.

Follow-on experiments should be primarily concerned with establishing threshold "crack", burning and motor conditions needed to initiate various propellants. Analysis is needed to establish the likelihood of achieving the threshold conditions.

REFERENCES

1. Takata, A. N., and A. Wiedermann, "Initiation Mechanisms of Solid Rocket Propellant Detonation", IITRI Interim Report for AFOSR, August 1976.

2. Takata, A. N., and A. Wiedermann, "Initiation Mechanisms of Solid Rocket Propellant Detonation", IITRI Second Interim Report for AFOSR, November 1977.

3. Takata, A. N., and A. Wiedermann, "Initiation Mechanisms of Solid Rocket Propellant Detonation", 14th JANNAF Combustion Meeting, Chemical Propulsion Information Agency Publication 292, December 1977.

4. Takata, A. N., "Initiation Mechanisms of Solid Rocket Propellant Detonation", IITRI Third Interim Report for AFOSR, December 1978.

5. Kuo, K. K., A. T. Chen, and T. R. Davis, "Transient Flame Spreading and Combustion Processes Inside a Solid Propellant Crack", The Pennsylvania State University, University Park, Pennsylvania, 1977.

6. Lenoir, J. M., and G. Robillard, "A Mathematical Method to Predict the Effects of Erosive Burning in Solid Propellant Rockets", 6th Symposium on Combustion, 1956.

7. King, M. K., "A Modification of the Composite Propellant Burning Model of Lenoir and Robillard", Combustion and Flame 24, pp 365-368, 1975.

8. Krier, H., J. S. Tien, W. A. Sirignamo, and M. Summerfeld, "Nonsteady Burning Phenomena of Solid Propellants: Theory and Experiments", AIAA J. 6(2), February 1968.

9. Nelson, C. W., "On Calculating Ignition of a Propellant Bed", Memorandum Report ARBRL-MR-02864, U.S. Army Research and Development Command, Ballistic Research Laboratory, September 1978.

10. Carslaw, H. S., and J. C. Jaeger, "Conduction of Heat in Solids", Oxford Press, 2nd ed., 1959.

11. Boggs, T. L., C. F. Price, D. E. Zurn, R. L. Derr, and E. J. Dibble, "The Self-Deflagration of Cyclotetramethylenetranitramine (HMX)", AIAA/SAE 13th Propulsion Conference, July 1977.

12. Beckstead, M. W., R. L. Derr, and C. F. Price, "The Combustion of Solid Monopropellants and Composite Propellants", 13th Symposium (International) on Combustion, pp 1047-1056, 1971.

13. Takata, A. N., W. Wulff, et al, "Study of the Behavior of Systems Containing High Explosives When Subject to Fire (U)", DASA Report 1833, July 1966.

14. Tomlinson, W. R. Jr., "Properties of Explosives of Military", Picatinny Arsenal, Technical Report 1740, April 1958.

15. de Longuiville, Y. C. Fauguignon, H. Moulard, "Initiation of Several Condensed Explosives by a Given Duration Shock Wave", Sixth Symposium (International) on Detonation, pp 16-24, August 1976.

APPENDIX: NOMENCLATURE AND HMX DATA

This appendix describes variables used in this report as well as the properties used for HMX and its reaction gases. The letter is presented in Table 3.

Nomenclature

a	rate of steady burning at 1 bar of pressure, cm/sec
C_g	specific heat of gases evolved by propellant at constant pressure, cal/g- K
C_m	specific heat of molten propellant, cal/g- K
C_p	specific heat of solid propellant, cal/g- K
C_w	crack width, cm
c_1, c_2	constants used to describe heat transfer coefficient h where $h = c_1(Z \exp - E/T_f)^{c_2}$
E	activation energy of propellant divided by gas constant, K
h	heat transfer coefficient associated with heat flux from foam to melt interface, cal/cm^2-sec- K
h_c	convective heat transfer coefficient, cal/cm^2-sec- K
h_{do}	initial altitude of driver before piston (see Figure 11), ft
h_g	height of gas space, cm
h_{go}	initial value of h_g (see Figure 11), cm
h_p	height of propellant cylinder, cm
h_{po}	initial value of h_p (see Figure 11), cm
I	mechanical impedence of solid propellant, equals I_o + 0.0002 P, bars-sec/cm
I_o	see I
k	constant used to predict erosive burning rate in equation (4), cm^3- K/cal

K	thermal conductivity of solid propellant, cal/cm-sec- K
L	indepth crack distance, cm
M_f	mass of unit area of foam layer, g/cm^2
M_w	molecular weight of reaction gases, g/mole
n	exponent of pressure P used to describe steady burning rate $\bar{r}_f$
P	gas pressure, bars or kbars
P_{max}	maximum value of P achieved, kbars
P_r	Prandtl number, dimensionless
$\bar{Q}_f$	sensible heat per unit mass of foam during steady burning, cal/g
Q_m	latent heat of fusion of propellant, cal/g
Q_r	heat of reaction of propellant gases cal/g
Q_s	heat generated within foam per unit mass of evolved gas, cal/g
q	heat flux incident upon propellant from external heat sources, cal/cm^2-sec
q_f	rate of heating of unit area of foam, cal/cm^2-sec
$\bar{q}_f$	steady value of q_f, cal/cm^2-sec
r_f	rate of propellant burning, cm/sec
$\bar{r}_f$	steady value of r_f at given pressure, cm/sec
R	gas constant, cm/ K
T_f	temperature of foam or propellant surface, K
$\bar{T}_f$	foam temperature during steady burning at given pressure, K
T_g	temperature of combustion gases, K
T_m	melt temperature of propellant, K
T_o	initial temperature of propellant, K
t	time, sec

t_i ignition time, sec

u cross flow gas velocity, cm/ms or cm/sec

W mass of driver (see Figure 11), lb

Z frequency factor, 1/sec

β constant used to describe erosive heating (see equation (10)), dimensionless

ρ density of solid propellant, g/cm^3

γ ratio of specific heats of combustion gases, dimensionless

TABLE 3. PROPERTIES OF HMX PROPELLANT AND GASES

Parameter	Value	Source
a, n	a = 0.030 cm/sec n = 0.86	Reference [12] Reference [12]
c_1, c_2	$c_1 = 7.6 \cdot 10^5$ cal/cm^2-sec- K c_2 = 0.338 (dimensionless)	Calculated [4] Calculated [4]
C_p	0.4 cal/g- K	Reference [13]
C_M	0.5 cal/g- K	Reference [13]
E	27,000 K	Reference [14]
I_o	0.450 bars-sec/cm	Assumed
K	0.0013 cal/cm-sec- K	Assumed
M_w	24.1 g/mole	Assumed
P_r	0.7 (dimensionless)	Calculated
Q_m	50 cal/g	Reference [13]
Q_r	1300 cal/g	Assumed
Q_s	150 cal/g	Assumed
R	3517 cm/ K	Assumed
T_m	555 K	Reference [13]
Z	$0.5 \cdot 10^{20}$/sec	Reference [14]
β	15 (dimensionless)	Assumed
ρ	1.9 g/cm^2	Reference [12]
γ	1.2 (dimensionless)	Assumed

DISTRIBUTION LIST

Aerojet Solid Propulsion Company
Attn: R. J. Schoner
Dept. 4320, Bldg 2019
P.O. Box 13400
Sacramento, CA 95813

Aerojet Solid Propulsion Company
Attn: R. L. Lovine
Dept. 4353
P.O. Box 13400
Sacramento, CA 95813

AFATL/DLDL
Attn: O. K. Heiney
Eglin AFB, FL 32542

AFRPL/DYSC
Attn: Mr. Andrepont
Dr. George
Edwards AFB, CA 93523

AFRPL/MKPA
Attn: Dr. Corley
Dr. Roberto
N. J. VanderHyde
Edwards AFB, CA 93523

AFRPL/MK
Attn: C. R. Cooke
Edwards AFB, CA 93523

A.R.A.P.
Attn: Dr. E. Stokes Fishburn
Mr. Hal Pergament
50 Washington Road
Princeton, NJ 08540

Atlantic Research Corporation
Attn: Merrill K. King
5390 Cherokee Avenue
Alexandria, VA 22030

AMXBR-IB
Attn: Dr. Ingo May
Dr. Kevin White
Aberdeen Proving Ground, MD 21005

U.S. Army Research Office
Attn: Mr. James J. Murray
Engineering Sciences Division
Box 12211
Research Triangle Park, NC 27709

Brigham Young University
Attn: L. Douglas Smoot
Dept. of Chemical Engineering
350B ESTB
Prove, UT 84602

California Institute of Technology
Attn: Prof. F.E.C. Culick
204 Karman Lab, 301-46
1201 E. California St.
Pasadena, CA 91109

University of Delaware
Attn: Dr. Thomas B. Brill
Dept. of Chemistry
Newark, Delaware 19711

EOARD
Attn: Maj Uhlig
Box 14
FPO New York 09510

Hercules Incorporated
Allegany Ballistics Laboratory
Attn: Dr. R. R. Miller
P.O. Box 210
Cumberland, MC 21502

Hercules Incorporated
Bacchus Works
Attn: Dr. Merrill W. Beckstead
P.O. Box 98
Magna, UT 84044

University of Illinois
Attn: Prof. Herman Krier
Prof. Roger A. Strehlow
Transportation Bldg
Urbana, IL 61801

U.S. Naval Weapons Center
Attn: Thom Boggs
Dr. Ronald L. Derr
Code 6082
China Lake, CA 93555

Office of Naval Research
Attn: Jim Patton, Code 473
Ballston Tower #1
800 N. Quincy St.
Arlington, VA 22217

The Pennsylvania State University
Attn: G. M. Faeth
Prof. Kenneth K. Kuo
Mechanical Engineering Building
University Park, PA 16802

Princeton University
Attn: L. H. Caveny
Martin Summerfield
Guggenheim Labs, Forrestal Campus
Princeton, NJ 08540

Rockwell International/Rocketdyne Div.
Attn: Mr. C. H. Burnside
William H. Miller
P.O. Box 548
McGregor, TX 76657

Stanford Research Institute
Attn: Dr. M. Cowperthwaite
Menlo Park, CA 94025

Thiokol/Huntsville Division
Attn: Dr. D. A. Flanigan
Dr. R. L. Glick
Huntsville, AL 35807

United Technologies Corporation
Attn: Robert S. Brown
Chemical Systems Division
1050 E. Arques Ave.
Sunnyvale, CA 94088

U.S. Naval Weapons Center
Attn: Thom Boggs
Dr. Ronald L. Derr
Code 6082
China Lake, CA 93555

Office of Naval Research
Attn: Jim Patton, Code 473
Ballston Tower #1
800 N. Quincy St.
Arlington, VA 22217

The Pennsylvania State University
Attn: G. M. Faeth
Prof. Kenneth K. Kuo
Mechanical Engineering Building
University Park, PA 16802

Princeton University
Attn: L. H. Caveny
Martin Summerfield
Guggenheim Labs, Forrestal Campus
Princeton, NJ 08540

Rockwell International/Rocketdyne Div.
Attn: Mr. C. H. Burnside
William H. Miller
P.O. Box 548
McGregor, TX 76657

Stanford Research Institute
Attn: Dr. M. Cowperthwaite
Menlo Park, CA 94025

Thiokol/Huntsville Division
Attn: Dr. D. A. Flanigan
Dr. R. L. Glick
Huntsville, AL 35807

United Technologies Corporation
Attn: Robert S. Brown
Chemical Systems Division
1050 E. Arques Ave.
Sunnyvale, CA 94088